Agent-based Modelling of Quantum Prisoner's Dilemma

Rajdeep Tah* and Colin Benjamin†
School of Physical Sciences, National Institute of Science Education and Research, HBNI, Jatni-752050, India and Homi Bhabha National Institute, Training School Complex, Anushakti Nagar, Mumbai, 400094, India

What happens when an infinite number of players play a quantum game? In this paper, we will answer this question by looking at the emergence of cooperation, in the presence of noise, in a one-shot quantum Prisoner's dilemma (QuPD). We will use the numerical Agent-based model (ABM), and compare it with the analytical Nash equilibrium mapping (NEM) technique. To measure cooperation, we consider five indicators, i.e., game magnetization, entanglement susceptibility, correlation, player's payoff average and payoff capacity, respectively. In quantum social dilemmas, entanglement plays a non-trivial role in determining the behaviour of the players in the thermodynamic limit, and for QuPD, we consider the existence of bipartite entanglement between neighbouring players. For the five indicators in question, we observe *first*-order phase transitions at two entanglement values, and these phase transition points depend on the payoffs associated with the QuPD game. We numerically analyze and study the properties of both the *Quantum* and the *Defect* phases of the QuPD via the five indicators. The results of this paper demonstrate that both ABM and NEM, in conjunction with the chosen five indicators, provide insightful information on cooperative behaviour in an infinite-player one-shot quantum Prisoner's dilemma.

I. INTRODUCTION

In the evolutionary context, when we think about examples of social dilemmas (SD), the first thing that comes to our mind is the classical Prisoner's dilemma (or, CPD)[1, 2]. In fact, it is one of the most popular game theoretic models out there that can be used to study a vast array of topics, involving both *one-shot* and *repeated* game settings (see, Refs. [3–5, 8, 9]). In CPD, as the word "*dilemma*" in the name suggests, the Nash equilibrium, i.e., a set of *actions* (or, *strategies*) that lead to an outcome deviating from which one gets worse payoffs, is the *Defect* strategy. This is surprising since there exists a *Pareto optimal* outcome, which for CPD, has better payoffs for both the players and is associated with the *Cooperate* strategy. The *Pareto optimal* strategy and the *Nash equilibrium* strategy are not the same. Till now, most research papers (see, Refs. [3, 10–13, 20]) have been largely restricted to CPD and on understanding how players behave in the *thermodynamic* (or, *infinite* population) *limit* (denoted as *TL*). However, much less focus has been given to the quantum counterpart of CPD, i.e., quantum Prisoner's dilemma (QuPD) in the *TL*. Previously, it was shown, in Refs. [3–5, 8, 9, 16, 18], that by quantizing the CPD (see, *Eisert-Wilkens-Lewenstein*, or EWL, protocol in Ref. [9]) and by introducing a unitary *quantum* strategy ($\mathbb{Q}$) in the modified CPD set-up, we can remove the *dilemma* associated with the CPD game. Further research works involving an infinite number of players (see, Refs. [3, 4, 8, 16]) have also shown that the QuPD game can help us understand the emergence of cooperation among the players. However, all these research works have an analytical, rather than a numerical, approach to understanding the question of the emergence of cooperative behaviour.

In this paper, we will numerically study and analyze how cooperative behaviour arises among an infinite number of players playing a *one-shot* QuPD game, and how entanglement (γ) affects them. To do so, we will take the help of five different indicators, namely, Game magnetization (μ), Entanglement susceptibility (χ_γ), Correlation ($\mathfrak{c}_j$), Player's payoff average ($\langle\Lambda\rangle$) and the Payoff capacity ($\wp_C$), all of them are analogues to the thermodynamic counterparts, i.e., Magnetization, Magnetic susceptibility, Correlation, average Internal energy (or, $\langle\mathbb{E}\rangle$) and the Specific heat capacity at constant volume (or, $\mathtt{C}_{\mathbb{V}}$), respectively. We will adopt a numerical Agent-based modelling (ABM) technique to study cooperative behaviour among players in the QuPD game, and we will compare our results with the analytical Nash equilibrium mapping (NEM) method. There exist other analytical methods, like Darwinian selection (DS) and Aggregate selection (AS), to analyze μ, χ_γ, $\mathfrak{c}_j$, $\langle\Lambda\rangle$ and $\wp_C$, in addition to NEM method. However, in a previous work (see, Ref. [13]), we have shown via a detailed calculation the incorrectness of these analytical methods. Hence, in this work, we will only compare the NEM with the numerical ABM, since both DS and AS are incorrect. Both ABM and NEM are based on the *1D*-Periodic Ising chain (or, IC) with nearest neighbour interactions (see, Refs. [7, 8, 11, 13]). Before moving further, we try to understand what the five aforementioned indicators actually mean. In a symmetric *2-player, 2-strategy* social dilemma game, 2 players (say, $\mathfrak{P}_1$ and $\mathfrak{P}_2$) have 2 different strategies $\$_1$ and $\$_2$ available at their disposal. Thus they have a choice between the two accessible strategies ($\$_1$ or $\$_2$), which could result in the same or different outcomes (aka, *payoffs*) for each of them. The *four* strategy sets for $\mathfrak{P}_1$ and $\mathfrak{P}_2$, i.e., $(\$|_{\mathfrak{P}_1},\ \$|_{\mathfrak{P}_2}) \in \{(\$_1,\$_1),\ (\$_2,\$_1),\ (\$_1,\$_2),\ (\$_2,\$_2)\}$, are each linked to the payoffs $(\mathrm{m},\mathrm{n},\mathrm{p},\mathrm{q})$ via the *symmetric*

* rajdeep.phys@gmail.com
† colin.nano@gmail.com

payoff matrix (Λ):

$$\Lambda = \begin{array}{c|cc} & \$_1 & \$_2 \\ \hline \$_1 & \mathrm{m,m} & \mathrm{n,p} \\ \$_2 & \mathrm{p,n} & \mathrm{q,q} \end{array}. \quad (1)$$

The *Game magnetization* (μ), analogous to the thermodynamic magnetization, is calculated by subtracting the number of players choosing $\$_2$ strategy from the number of players choosing $\$_1$ strategy. The *Entanglement susceptibility* provides the variation in the rate of change in μ, owing to a change in the entanglement γ. *Correlation* indicates how closely two players' strategies, at two separate sites, correlate with one another, while the individual player's payoff average, the analogue of $\langle \mathbb{E} \rangle$ for thermodynamic systems, is simply the average payoff that a player receives after playing the game in a *one-shot* environment. Finally, *Payoff capacity*, the analogue of $\mathtt{C}_{\mathbb{V}}$ for thermodynamic systems, indicates the amount the player's payoff changes for a unit change in *noise*. The *uncertainty* associated with the selection of a strategy by a player is termed *noise*.

A brief introduction to CPD and QuPD, along with a note on NEM and ABM, is presented in Sec. II, wherein, we will also understand how QuPD can be mapped to the $1D$-Ising chain (or, IC). In QuPD, for all the five indicators in question, we find that ABM and NEM results exactly match with each other, and they clearly predict the entanglement γ range (defined by two critical γ values: γ_A and γ_B) in between which, i.e., for $\gamma \in [\gamma_A, \gamma_B]$, *quantum* becomes the dominant strategy. For all indicators we observe an interesting phenomenon of two *first*-order phase transitions, namely, the change of strategies from *Defect* ($\mathcal{D}$) $\rightarrow$ *Quantum* ($\mathbb{Q}$) (at entanglement value γ_A) and $\mathbb{Q} \rightarrow \mathcal{D}$ (at entanglement value γ_B), regardless of noise in the system. This result is very similar to that observed in Type-*I* superconductors, at a certain critical temperature and in the absence of an external field (see, Refs. [3, 21]). This also showcases the fact that for QuPD, at finite entanglement γ and *zero* noise, we observe a change in the Nash equilibrium condition from *All*-$\mathcal{D}$ to *All*-$\mathbb{Q}$ and this is marked by a *first*-order phase transition in all the indicators. After analyzing the results obtained for all five indicators via ABM and NEM, we see that all five indicators can identify the phase transition, occurring at two different values of entanglement, i.e., γ_A and γ_B, in QuPD. Remarkably, at finite entanglement, we also see that all five indicators show a phase transition as a function of payoffs too.

The organization of the paper is as follows: In Sec. II, we will discuss both CPD and QuPD, followed by a detailed description of the mathematical framework of NEM and the algorithm of ABM, and how we map our QuPD game to the *1D*-IC. Then, in Sec. III, we will discuss and analyze the results obtained for all the five indicators in question, in the *TL*, and finally, we conclude our paper by summarizing all the important observations from our work in Sec. IV.

II. THEORY

Here, we will discuss both *Classical* and *Quantum* Prisoner's dilemma (PD), followed by a brief introduction to the analytical *Nash equilibrium mapping* (NEM) technique, and finally, we will conclude this section by discussing the algorithm associated to the numerical *Agent-based modelling* (ABM). Both NEM and ABM are based on the exactly solvable $1D$-IC, and instead of dealing with dynamical strategy evolutions, we involve equilibrium statistical mechanics. Hence, we consider a *one-shot* PD game in the infinite-player limit, for both Classical and Quantum cases.

A. Classical Prisoner's Dilemma (CPD)

In CPD [1, 2], as the name suggests, two *independent* players (say, $\mathfrak{P}_1$ and $\mathfrak{P}_2$), accused of committing a crime, are being interrogated by the law agencies, and they have either option to *Cooperate* ($\mathfrak{C}$) with each other or *Defect* ($\mathfrak{D}$). If both players opt for $\mathfrak{C}$-strategy, then they are rewarded with a payoff $\mathbb{R}$, whereas, if both choose $\mathfrak{D}$-strategy, then they get the punishment payoff $\mathbb{P}$. However, if both $\mathfrak{P}_1$ and $\mathfrak{P}_2$ choose opposite strategies, then the one choosing $\mathfrak{C}$-strategy gets the *sucker's* payoff $\mathbb{S}$, and the one choosing $\mathfrak{D}$-strategy gets the temptation payoff $\mathbb{T}$, respectively. The payoffs have to fulfil the criteria: $\mathbb{T} > \mathbb{R} > \mathbb{P} > \mathbb{S}$. Hence, the CPD payoff matrix ($\tilde{\Xi}$) is,

$$\tilde{\Xi} = \begin{array}{c|cc} & \mathfrak{C} & \mathfrak{D} \\ \hline \mathfrak{C} & \mathbb{R},\mathbb{R} & \mathbb{S},\mathbb{T} \\ \mathfrak{D} & \mathbb{T},\mathbb{S} & \mathbb{P},\mathbb{P} \end{array}. \quad (2)$$

From $\tilde{\Xi}$ in Eq. (2), one would think that the two rational players, who are always looking for payoff maximization, would choose the Pareto optimal $\mathfrak{C}$-strategy since it is a *win-win* situation for both. However, owing to independence in strategy selection, both $\mathfrak{P}_1$ and $\mathfrak{P}_2$ choose the $\mathfrak{D}$-strategy (thus the name "*dilemma*") to ensure that none of them receives the minimum payoff, i.e., the sucker's payoff $\mathbb{S}$, due to a unilateral change in the opponent's strategy. Hence, the Nash equilibrium in CPD is $\mathfrak{D}$. For our case, we rewrite the CPD payoffs $\{\mathbb{R}, \mathbb{S}, \mathbb{T}, \mathbb{P}\}$ in terms of a new set of payoffs: Cooperation bonus ($\mathbb{B}$) and Cost ($\mathbb{C}$), where we redefine $\mathbb{R} = \mathbb{B} - \mathbb{C}$ (i.e., cooperation bonus with the cost subtracted out), $\mathbb{T} = \mathbb{B}$ (or, the entire Cooperation bonus), $\mathbb{S} = -\mathbb{C}$ (i.e., bearing the cost without any bonus) and $\mathbb{P} = 0$, respectively. Here, $\mathbb{B} \geq \mathbb{C} \geq 0$, with $\mathbb{B} \geq (\mathbb{B} - \mathbb{C}) \geq 0 \geq -\mathbb{C}$ (i.e., $\mathbb{T} > \mathbb{R} > \mathbb{P} > \mathbb{S}$ criteria is satisfied in this case also), and we will be using the same $\{\mathbb{B}, \mathbb{C}\}$ as our payoffs when we deal with the quantum Prisoner's dilemma in the next section.

B. Quantum Prisoner's Dilemma (QuPD)

The topic of extending the framework of CPD to the quantum regime is discussed elaborately in Refs. [3–5, 9]. Still, we will discuss them in this paper for the reader's convenience. The players in CPD, say $\mathfrak{P}_1$ and $\mathfrak{P}_2$, are now treated as *qubits* in QuPD, and the state of the qubits represent the strategies adopted by the players. Analogous to CPD, in QuPD, the *Cooperate*-strategy is denoted by $|\mathfrak{C}\rangle$ and the *Defect*-strategy is denoted by $|\mathfrak{D}\rangle$, respectively. Note that even though the players are denoted by *qubits*, the strategies available to the players are still classical in nature. Here,

$$|\mathfrak{C}\rangle = [1 \;\; 0]^{\perp}, \text{ and } |\mathfrak{D}\rangle = [0 \;\; 1]^{\perp}, \tag{3}$$

where, $\perp$ denotes *transpose* of the given row matrices. The strategy to be adopted by every player is given by acting the unitary operator [9],

$$\hat{\mathfrak{U}}(\varphi,\vartheta) = \begin{bmatrix} e^{i\varphi}\cos\left(\frac{\vartheta}{2}\right) & \sin\left(\frac{\vartheta}{2}\right) \\ -\sin\left(\frac{\vartheta}{2}\right) & e^{-i\varphi}\cos\left(\frac{\vartheta}{2}\right) \end{bmatrix}, \tag{4}$$

on the initial state of the players. The operator $\hat{\mathfrak{U}}(\varphi,\vartheta)$ $\forall\ \vartheta \in [0,\pi]$, $\varphi \in [0,\frac{\pi}{2}]$, acts independently on the individual Hilbert spaces of both players. Here, $\hat{\mathfrak{U}}(\varphi = 0, \vartheta = 0) = \hat{\mathbb{I}}_{2\times 2}$ (i.e., *Identity* operator) represents the *cooperation* strategy, and

$$\hat{\mathfrak{U}}(\varphi = 0, \vartheta = \pi) = \begin{bmatrix} 0 & 1 \\ -1 & 0 \end{bmatrix},$$

represents the *defection* strategy [3, 9]. Since we are dealing with QuPD, the concept of *entanglement* comes into the picture, and before any strategy-modification operation, the two *distinct*, *individual* qubits of the two players are entangled via the *unitary* entanglement operator [9],

$$\hat{\Gamma}(\gamma) = \left(\cos\frac{\gamma}{2}\right)\hat{\mathbb{I}}\otimes\hat{\mathbb{I}} - \left(i\sin\frac{\gamma}{2}\right)\hat{\mathfrak{S}}_Y\otimes\hat{\mathfrak{S}}_Y, \tag{5}$$

where, $\hat{\mathbb{I}}$ is the 2×2 Identity operator, $\hat{\mathfrak{S}}_Y = \begin{bmatrix} 0 & -i \\ i & 0 \end{bmatrix}$ is the *Pauli-Y* operator, and γ denotes the *entanglement parameter* in QuPD, i.e., for $\gamma = \frac{\pi}{2}$, we have *maximal* entanglement and for $\gamma = 0$, we have *minimal* entanglement. Both the players are well aware of the entanglement operator $\hat{\Gamma}(\gamma)$. If both the *players/qubits* (say, $\mathfrak{P}_1$ and $\mathfrak{P}_2$) choose $|\mathfrak{C}\rangle$ as their initial states and $\hat{\Gamma}(\gamma)$ acting on them gives the entangled state (from, Eq. (5)) [9],

$$|\alpha\rangle = \hat{\Gamma}(\gamma)|\mathfrak{C}\mathfrak{C}\rangle = \cos\frac{\gamma}{2}|\mathfrak{C}\mathfrak{C}\rangle + i\sin\frac{\gamma}{2}|\mathfrak{D}\mathfrak{D}\rangle. \tag{6}$$

Subsequently, both players apply $\hat{\mathfrak{U}}(\varphi,\vartheta)$ on their respective qubits, giving us the intermediate state [9],

$$|\beta\rangle = \hat{\mathfrak{U}}(\varphi_{\mathfrak{P}_1},\vartheta_{\mathfrak{P}_1})\otimes\hat{\mathfrak{U}}(\varphi_{\mathfrak{P}_2},\vartheta_{\mathfrak{P}_2})\hat{\Gamma}(\gamma)|\mathfrak{C}\mathfrak{C}\rangle. \tag{7}$$

Finally, before any measurement is made, the disentangling operator $\hat{\Gamma}^{\dagger}(\gamma)$ is acted on $|\beta\rangle$, given in Eq. (7), and the final non-entangled state is given as [9],

$$|\mathbb{F}\rangle = \hat{\Gamma}^{\dagger}(\gamma)\hat{\mathfrak{U}}(\varphi_{\mathfrak{P}_1},\vartheta_{\mathfrak{P}_1})\otimes\hat{\mathfrak{U}}(\varphi_{\mathfrak{P}_2},\vartheta_{\mathfrak{P}_2})\hat{\Gamma}(\gamma)|\mathfrak{C}\mathfrak{C}\rangle. \tag{8}$$

Similar to CPD, we can determine the game payoffs for QuPD by projecting the final non-entangled state $|\mathbb{F}\rangle$ onto the basis vectors that entirely span the combined Hilbert space of the two-players, i.e., $|\mathfrak{C}\mathfrak{C}\rangle$, $|\mathfrak{D}\mathfrak{D}\rangle$, $|\mathfrak{C}\mathfrak{D}\rangle$ and $|\mathfrak{D}\mathfrak{C}\rangle$, respectively. These values, coupled with the CPD payoffs (see, Eq. (2) and new payoffs $\mathbb{B},\mathbb{C}$), give us the QuPD payoffs (Λ) for both players: $\mathfrak{P}_1$ and $\mathfrak{P}_2$, as,

$$\Lambda_{\mathfrak{P}_1} = (\mathbb{B}-\mathbb{C})\sigma_{\mathfrak{C}\mathfrak{C}} - \mathbb{C}\sigma_{\mathfrak{C}\mathfrak{D}} + \mathbb{B}\sigma_{\mathfrak{D}\mathfrak{C}} + \cancelto{0}{\mathbb{P}}\sigma_{\mathfrak{D}\mathfrak{D}} \tag{9}$$

$$\Lambda_{\mathfrak{P}_2} = (\mathbb{B}-\mathbb{C})\sigma_{\mathfrak{C}\mathfrak{C}} - \mathbb{C}\sigma_{\mathfrak{D}\mathfrak{C}} + \mathbb{B}\sigma_{\mathfrak{C}\mathfrak{D}} + \cancelto{0}{\mathbb{P}}\sigma_{\mathfrak{D}\mathfrak{D}} \tag{10}$$

where, $\sigma_{\mathfrak{C}\mathfrak{C}} = |\langle\mathbb{F}|\mathfrak{C}\mathfrak{C}\rangle|^2$, $\sigma_{\mathfrak{C}\mathfrak{D}} = |\langle\mathbb{F}|\mathfrak{C}\mathfrak{D}\rangle|^2$, $\sigma_{\mathfrak{D}\mathfrak{C}} = |\langle\mathbb{F}|\mathfrak{D}\mathfrak{C}\rangle|^2$, and $\sigma_{\mathfrak{D}\mathfrak{D}} = |\langle\mathbb{F}|\mathfrak{D}\mathfrak{D}\rangle|^2$, respectively. By introducing a *Quantum* strategy operator [3], $\hat{\mathbb{Q}} = i\hat{\mathfrak{S}}_Z = \hat{\mathfrak{U}}(\varphi = \frac{\pi}{2}, \vartheta = 0)$, where, $\hat{\mathfrak{S}}_Z = \begin{bmatrix} 1 & 0 \\ 0 & -1 \end{bmatrix}$ is the *Pauli-Z* operator, we have the players opting for a different strategy than the available classical strategies $\mathfrak{C}$ and $\mathfrak{D}$. Initially, superposition states like $\frac{1}{\sqrt{2}}(|\mathfrak{C}\rangle + |\mathfrak{D}\rangle)$ used to remain invariant under the action of classical strategies. However, upon the action of $\hat{\mathbb{Q}}$ on $\frac{1}{\sqrt{2}}(|\mathfrak{C}\rangle + |\mathfrak{D}\rangle)$, we get an orthogonal state $\frac{1}{\sqrt{2}}e^{i\pi/2}(|\mathfrak{C}\rangle - |\mathfrak{D}\rangle)$, where $e^{i\pi/2}$ is a global phase factor. In QPD, we involve both quantum and classical strategies, and the payoff matrix is:

$$\tilde{\Lambda} = \left[\begin{array}{c|ccc} & \mathfrak{C} & \mathfrak{D} & \mathbb{Q} \\ \hline \mathfrak{C} & \mathbb{B}-\mathbb{C},\mathbb{B}-\mathbb{C} & -\mathbb{C},\mathbb{B} & \mathfrak{L}_1,\mathfrak{L}_1 \\ \mathfrak{D} & \mathbb{B},-\mathbb{C} & 0,0 & \mathfrak{L}_3,\mathfrak{L}_2 \\ \mathbb{Q} & \mathfrak{L}_1,\mathfrak{L}_1 & \mathfrak{L}_2,\mathfrak{L}_3 & \mathbb{B}-\mathbb{C},\mathbb{B}-\mathbb{C} \end{array}\right]. \tag{11}$$

where, $\mathfrak{L}_1 = (\mathbb{B}-\mathbb{C})\cos^2\gamma$, $\mathfrak{L}_2 = -\mathbb{C}\cos^2\gamma + \mathbb{B}\sin^2\gamma$, and $\mathfrak{L}_3 = \mathbb{B}\cos^2\gamma - \mathbb{C}\sin^2\gamma$. Hence, QPD is a *three*-strategy game, but it is difficult to map the *three*-strategy QuPD to an exactly solvable *spin-1* IC [3]. However, previous works on QuPD (see, Refs. [3, 5, 9]) have shown how $\mathbb{Q}$ fare against the classical strategies $\mathfrak{C}$ and $\mathfrak{D}$, indicating that it will be a wiser choice to divide our *three*-strategy QuPD into two *two*-strategy QuPD problems (so that we can map them individually to a *spin-1/2* IC), and we can compare the ($\mathbb{Q}$ vs $\mathfrak{D}$) as well as the ($\mathbb{Q}$ vs $\mathfrak{C}$) cases. As visualized in Fig. 1, for each case of the *two*-strategy QuPD, we have two entangled players (playing the *two*-strategy QuPD) at every site of the infinitely long $1D$-IC (i.e., the *thermodynamic* limit), and each site is coupled to its nearest neighbouring sites via the coupling constant $\mathcal{T}$. All the sites, each consisting of two entangled players, are subjected to a uniform external field $\mathcal{F}$ (analogous to the external magnetic field Ising factor). From Eq. (11), one can notice from the given payoff matrix Λ that for ($\mathbb{Q}$ vs $\mathfrak{C}$) case, both ($\mathbb{Q},\mathbb{Q}$) and ($\mathfrak{C},\mathfrak{C}$) strategy pairs gives

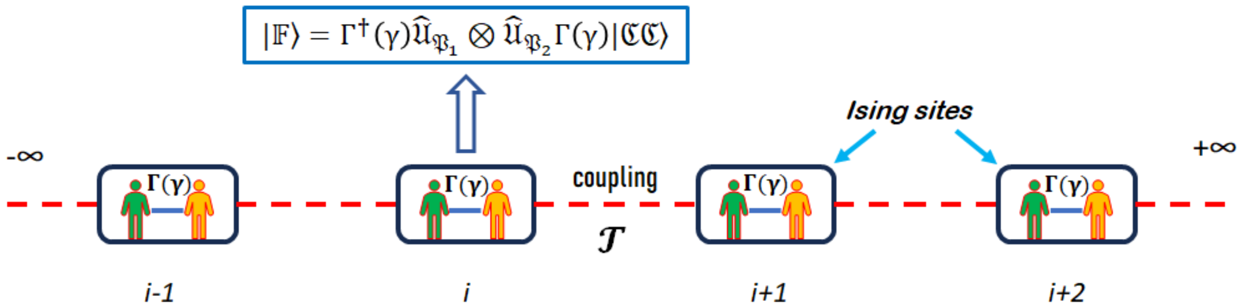

FIG. 1: **NEM/ABM**: Visualization of QuPD in thermodynamic (or, *infinite-player*) limit. The QuPD game is mapped to a $1D$-Ising chain, where at each site, two entangled players reside, and they play the *two*-strategy QuPD. The players also interact with their nearest neighbours via a classical coupling $\mathcal{T}$, in the presence of an external uniform field $\mathcal{F}$ and *noise* β.

the same payoff to both the players, and we observe no payoff variations when switching from classical to quantum strategies. Owing to this, we only consider the ($\mathbb{Q}$ vs $\mathfrak{D}$) case for our further work.

For ($\mathbb{Q}$ vs $\mathfrak{D}$) case, we have the 2×2-reduced payoff matrix for a single player (say, the *row* player) as,

$$\Lambda = \left[\begin{array}{c|cc} & \mathbb{Q} & \mathfrak{D} \\ \hline \mathbb{Q} & (\mathbb{B}-\mathbb{C}) & (\mathbb{B}\sin^2\gamma - \mathbb{C}\cos^2\gamma) \\ \mathfrak{D} & (\mathbb{B}\cos^2\gamma - \mathbb{C}\sin^2\gamma) & 0 \end{array}\right]. \tag{12}$$

This Λ, in Eq. (12), will be utilised in our further calculations in the thermodynamic limit. In the next section, we will discuss the analytical NEM very briefly, and we will compare the results from NEM with the results of numerical ABM.

1. Nash equilibrium mapping (NEM)

In one of our previous works (see, Ref. [13]), we have discussed the mathematical framework of NEM in great detail. To summarize for the readers, in NEM, we analytically map a SD to a *spin-1/2* infinitely long $1D$-IC (i.e., the *TL*) (see, Refs. [7, 11, 13]). Initially, we consider a 2-strategy; 2-player SD while mapping it to a 2-site IC. The 2 strategies (say, $\$_1$ and $\$_2$) have a *one-to-one* mapping to the *2*-spin (say, ± 1) $1D$-IC and we have the 2-site (say, A and B) $1D$-IC Hamiltonian as [13],

$$H = -\mathcal{T}(\sigma_A\sigma_B + \sigma_B\sigma_A) - \mathcal{F}(\sigma_A + \sigma_B) = \Delta_A + \Delta_B, \tag{13}$$

where, $\mathcal{T}$ is the coupling constant, $\mathcal{F}$ is the external field, $\sigma_i\ \forall\ i \in \{A, B\}$, is the spin (either $+1$ or -1) at the i^{th} site, and Δ_i denotes the energy of the i^{th} site. Each of the individual site's energy is given as,

$$\Delta_A = -\mathcal{T}\sigma_A\sigma_B - \mathcal{F}\sigma_A, \text{ and } \Delta_B = -\mathcal{T}\sigma_B\sigma_A - \mathcal{F}\sigma_B. \tag{14}$$

Here, the total two-spin IC energy: $\Delta = \Delta_A + \Delta_B$. In social dilemmas, the maximization of the player's feasible payoffs corresponds to finding the Nash equilibrium of the game. However, when we consider a $1D$-IC, we look to lessen the Δ in order to reach the energy equilibrium condition. Hence, in order to establish a link between the IC's energy equilibrium configuration and the Nash equilibrium of a SD, we equate the SD payoff matrix to the negative of the energy matrix [7]. Each element of Δ (i.e., Δ_i) corresponds to a particular pair of spin values (σ_A, σ_B), i.e., $(\sigma_A, \sigma_B) \in \{(\pm 1, \pm 1)\}$, at each $1D$-IC site since game payoff maximization indicates negative energy minimization. Thus,

$$-\Delta = \left[\begin{array}{c|cc} & \sigma_B = +1 & \sigma_B = -1 \\ \hline \sigma_A = +1 & (\mathcal{T}+\mathcal{F}), (\mathcal{T}+\mathcal{F}) & (\mathcal{F}-\mathcal{T}), -(\mathcal{F}+\mathcal{T}) \\ \sigma_A = -1 & -(\mathcal{F}+\mathcal{T}), (\mathcal{F}-\mathcal{T}) & (\mathcal{T}-\mathcal{F}), (\mathcal{T}-\mathcal{F}) \end{array}\right]. \tag{15}$$

For a 2-player; 2-strategy (say, $\$_1$ and $\$_2$) *symmetric* SD game, we have the SD payoff matrix Λ' as,

$$\Lambda' = \left[\begin{array}{c|cc} & \$_1 & \$_2 \\ \hline \$_1 & \mathrm{m},\mathrm{m} & \mathrm{n},\mathrm{p} \\ \$_2 & \mathrm{p},\mathrm{n} & \mathrm{q},\mathrm{q} \end{array}\right]. \tag{16}$$

where, $(\mathrm{m}, \mathrm{n}, \mathrm{p}, \mathrm{q})$ are defined as the SD payoffs. Using a set of linear transformations on Λ' in Eq. (16), to establish a *one-to-one* correspondence between the payoffs in Eq. (16) and the energy matrix Δ of the two-spin Ising chain in Eq. (15), that preserves the Nash equilibrium (see, Ref. [7] and **Appendix** of Ref. [6] for detailed calculations),

$$\mathrm{m} \to \frac{\mathrm{m}-\mathrm{p}}{2},\ \mathrm{n} \to \frac{\mathrm{n}-\mathrm{q}}{2},\ \mathrm{p} \to \frac{\mathrm{p}-\mathrm{m}}{2},\ \mathrm{q} \to \frac{\mathrm{q}-\mathrm{n}}{2}, \tag{17}$$

we equate Λ' (see, Eq. (16)) to $-\Delta$ (see, Eq. (15)), to rewrite the Ising parameters $(\mathcal{T}, \mathcal{F})$ in terms of the SD payoffs as [7, 11, 13],

$$\mathcal{F} = \frac{(\mathrm{m}-\mathrm{p}) + (\mathrm{n}-\mathrm{q})}{4}, \text{ and } \mathcal{T} = \frac{(\mathrm{m}-\mathrm{p}) - (\mathrm{n}-\mathrm{q})}{4}. \tag{18}$$

In $1D$-IC, the parameter β is defined as proportional to the temperature (T) inverse, or, $\beta = \frac{1}{k_B T}$, where k_B is the *Boltzmann constant*, and in game theoretic models, temperature implies *uncertainty* in player's strategy selection, and this is termed as *noise*. Therefore, $T \to 0$ (or, $\beta \to \infty$) implies *zero noise* (denoted by Z-N), i.e., no change in the players' strategies, whereas, $T \to \infty$ (or, $\beta \to 0$) implies *infinite noise* (denoted by I-N), i.e., complete randomness in the player's strategy selection. We can also interpret β as the *selection intensity* (see, Ref. [14]) where, for $\beta \ll 1$, we observe strategies being selected at random, whereas, for $\beta \gg 1$, we have a vanishing randomness in strategy selection.

For the given H (see, Eq. (13)) and Eq. (18), the partition function Υ^{NEM} can be written in terms of the SD parameters $(\mathrm{m}, \mathrm{n}, \mathrm{p}, \mathrm{q})$ as [13],

$$\Upsilon^{Ising} = \sum_{\{\sigma_i\}} e^{-\beta H} = e^{2\beta(\mathcal{T}+\mathcal{F})} + e^{2\beta(\mathcal{T}-\mathcal{F})} + 2e^{-2\beta\mathcal{T}},$$
$$\text{or, } \Upsilon^{NEM} = e^{\beta(\mathrm{m}-\mathrm{p})} + e^{-\beta(\mathrm{n}+\mathrm{q})} + 2e^{\frac{\beta}{2}(\mathrm{n}+\mathrm{p}-\mathrm{m}-\mathrm{q})}, \quad (19)$$

where, $\beta = \frac{1}{k_B T}$. For ($\mathbb{Q}$ vs $\mathfrak{D}$) case of QuPD, from Eq. (12), we have:

$$\mathrm{m} = (\mathbb{B} - \mathbb{C}); \quad \mathrm{n} = (\mathbb{B}\sin^2\gamma - \mathbb{C}\cos^2\gamma);$$
$$\mathrm{p} = (\mathbb{B}\cos^2\gamma - \mathbb{C}\sin^2\gamma); \quad \text{and} \quad \mathrm{q} = 0. \quad (20)$$

Hence, from Eqs. (18, 20), we have $(\mathcal{T}, \mathcal{F})$ in terms of the SD payoffs $(\mathbb{B}, \mathbb{C})$ and entanglement γ as,

$$\mathcal{T} = 0, \quad \text{and} \quad \mathcal{F} = \frac{(\mathbb{B}\sin^2\gamma - \mathbb{C}\cos^2\gamma)}{2} \quad (21)$$

The readers can refer to our previous work, involving NEM; ABM and other analytical methods, in Ref. [13], where the detailed calculations on deriving the analytical expressions for the given five indicators of cooperative behaviour: game magnetization (μ^{NEM}), entanglement susceptibility (χ_γ^{NEM}), correlation ($\mathfrak{c}_j^{NEM}$), player's payoff average ($\langle\Lambda\rangle^{NEM}$) and payoff capacity ($\wp_C^{NEM}$), with regards to two different classical SD (Hawk-Dove game and Public goods game) are shown. The same technique, as in Ref. [13], is followed here. So, we have the analytical expressions for the five different indicators for QuPD, in the thermodynamic (or, *infinite players*) limit, as,

1. Game magnetization: Using the Λ in Eq. (12) and Υ^{NEM} (see, Eqs. (19, 21)), we have the QuPD average game magnetization μ^{NEM} in the TL as,

$$\mu^{NEM} = \frac{1}{\beta}\frac{\partial}{\partial\mathcal{F}}\ln\Upsilon^{NEM} = \frac{\sinh\beta\mathcal{F}}{\sqrt{e^{-4\beta\mathcal{T}} + \sinh^2\beta\mathcal{F}}},$$
$$\text{or, } \mu^{NEM} = \frac{\sinh\left[\frac{\beta}{2}(\mathbb{B}\sin^2\gamma - \mathbb{C}\cos^2\gamma)\right]}{\mathfrak{W}}, \quad (22)$$

where, $\mathfrak{W} = \sqrt{\sinh^2[\frac{\beta}{2}(\mathbb{B}\sin^2\gamma - \mathbb{C}\cos^2\gamma)] + 1}$, respectively. Here, $\mathbb{B}$ is the Cooperation bonus, $\mathbb{C}$ is the cost, and γ denotes the entanglement associated with the QuPD game.

2. Entanglement susceptibility: To derive the analytical expression for the QuPD Entanglement susceptibility χ_γ^{NEM}, we partially differentiate μ^{NEM} with the entanglement parameter γ and normalize it by β, i.e.,

$$\chi_\gamma^{NEM} = \frac{1}{\beta}\frac{\partial}{\partial\gamma}\mu^{NEM}, \text{ for } \gamma \in [0,\pi],$$
$$\text{or, } \chi_\gamma^{NEM} = \frac{(\mathbb{B}+\mathbb{C})}{2}\cdot\frac{\sin(2\gamma)\cosh(\beta\mathcal{N})}{(1+\sinh^2\beta\mathcal{N})^{\frac{3}{2}}}, \quad (23)$$

where, $\mathcal{N} = \frac{1}{2}(\mathbb{B}\sin^2\gamma - \mathbb{C}\cos^2\gamma)$, respectively.

3. Correlation: In our previous work in Ref. [13], we derived the analytical NEM expression for the correlation $\mathfrak{c}_j^{NEM} (= \langle\sigma_i\sigma_{i+j}\rangle)$ between two sites separated by a distance j, for classical social dilemmas (CSD), as,

$$\mathfrak{c}_j^{NEM}\Big|_{CSD} = \cos^2\varphi + \left(\frac{\Omega_-}{\Omega_+}\right)^j \sin^2\varphi, \quad (24)$$

with $\cos^2\varphi = \frac{\sinh^2\beta\mathcal{F}}{\mathfrak{Y}}$, $\Omega_\pm = e^{\beta\mathcal{T}}[\cosh(\beta\mathcal{F}) \pm \sqrt{\mathfrak{Y}}]$, where $\mathfrak{Y} = \sinh^2\beta\mathcal{F} + e^{-4\beta\mathcal{T}}$. In QuPD, the calculation for correlation is very similar, where we just replace the $(\mathcal{T}, \mathcal{F})$ given in Eq. (24) with the values given in Eq. (21) to have the expression for the QuPD correlation $\mathfrak{c}_j^{NEM} = \langle\sigma_i\sigma_{i+j}\rangle$ as,

$$\mathfrak{c}_j^{NEM} = \cos^2\Phi + \left(\frac{\omega_-}{\omega_+}\right)^j \sin^2\Phi, \quad (25)$$

where, j is the *distance* between the two sites and

$$\cos^2\Phi = \frac{\sinh^2\beta\mathcal{N}}{\mathfrak{W}^2}, \quad \omega_\pm = [\cosh(\beta\mathcal{N}) \pm \mathfrak{W}], \quad (26)$$
$$\text{with, } \mathfrak{W} = \sqrt{\sinh^2[\frac{\beta}{2}(\mathbb{B}\sin^2\gamma - \mathbb{C}\cos^2\gamma)] + 1},$$
$$\text{and } \mathcal{N} = \frac{1}{2}(\mathbb{B}\sin^2\gamma - \mathbb{C}\cos^2\gamma). \quad (27)$$

4. Player's payoff average: The analytical expression for $\langle\Lambda\rangle^{NEM}$ in QuPD can be derived using Υ^{NEM} given in Eq. (19) as,

$$\Upsilon^{NEM} = e^{\beta(\mathrm{m}-\mathrm{p})} + e^{-\beta(\mathrm{n}+\mathrm{q})} + 2e^{\frac{\beta}{2}(\mathrm{n}+\mathrm{p}-\mathrm{m}-\mathrm{q})},$$
$$\text{or, } \Upsilon^{NEM} = e^{\beta(\mathbb{B}\sin^2\gamma - \mathbb{C}\cos^2\gamma)} + e^{\beta(\mathbb{C}\cos^2\gamma - \mathbb{B}\sin^2\gamma)} + 1.$$
$$\text{Thus, } \langle\Lambda\rangle^{NEM} = -\frac{1}{2}\langle\mathbb{E}\rangle^{NEM} = \frac{1}{2}\left[\frac{1}{\Upsilon^{NEM}}\frac{\partial\Upsilon^{NEM}}{\partial\beta}\right],$$
$$\text{or, } \langle\Lambda\rangle^{NEM} = \frac{\mathcal{N}(e^{2\beta\mathcal{N}} - e^{-2\beta\mathcal{N}})}{(1 + e^{2\beta\mathcal{N}} + e^{-2\beta\mathcal{N}})}, \quad (28)$$

where, $\langle\mathbb{E}\rangle$ denotes the average internal energy (**NOTE**: we take the $-ve$ of $\langle\mathbb{E}\rangle$ to maximize $\langle\Lambda\rangle$) and $\mathcal{N} = \frac{1}{2}(\mathbb{B}\sin^2\gamma - \mathbb{C}\cos^2\gamma)$, respectively.

5. Payoff capacity: The analytical expression for

$\wp_C^{NEM}$ in QuPD can also be derived from Υ^{NEM} given in Eqs. (19, 21, 28) as,

$$\Upsilon^{NEM} = e^{\beta(\mathbb{B}\sin^2\gamma - \mathbb{C}\cos^2\gamma)} + e^{\beta(\mathbb{C}\cos^2\gamma - \mathbb{B}\sin^2\gamma)} + 1.$$

Since the payoff capacity $\wp_C$ is analogous to the normalized thermodynamic specific heat capacity, at constant volume, $\mathtt{C}_{\mathbb{V}}$ (see, Ref. [13, 15, 22–24]), we have the analytical NEM expression for $\wp_C$, normalized by β^2, as,

$$\wp_C^{NEM} = \frac{1}{2\beta^2}\frac{\partial}{\partial\beta}\left[\frac{1}{\Upsilon^{NEM}}\frac{\partial\Upsilon^{NEM}}{\partial\beta}\right],$$
$$\text{or,}\;\; \wp_C^{NEM} = 2\mathcal{N}^2\frac{e^{2\beta\mathcal{N}}(1+4e^{2\beta\mathcal{N}}+e^{4\beta\mathcal{N}})}{(1+e^{2\beta\mathcal{N}}+e^{4\beta\mathcal{N}})^2}, \quad (29)$$

where, $\mathcal{N} = \frac{1}{2}(\mathbb{B}\sin^2\gamma - \mathbb{C}\cos^2\gamma)$. We will study the variation of these *five* indicators with respect to a changing $\gamma \in [0, \pi]$ while keeping $\mathbb{B} = 5.0$ and $\mathbb{C} = 2.0$ (i.e., constant values). In the next section, we will discuss the algorithm for Agent-based modelling.

2. *Agent-based Modelling (ABM)*

ABM [11, 13] is a numerical modelling technique often used to study classical SD in the *TL*. However, to the best of our knowledge, ABM has not been previously implemented to study the emergence of cooperative behaviour in quantum social dilemmas like QuPD, etc. Hence, the main attraction of our work is that we numerically analyze the emergence of cooperation among an infinite number of players, in the presence of entanglement γ. We consider a *1000* players, and these players reside on the $1D$-IC where each site consists of two entangled players, playing the *two*-strategy QuPD, and they interact with their nearest neighbours only, in the presence of a periodic boundary condition. The energy matrix Δ is just the negative of the QuPD payoff matrix Λ given in Eq. (12), and this gives the IC's individual site energy. At this point, we modify the player's strategy by iterating through a conditional loop *1,000,000* times, which amounts to an average of *1000* strategy modifications per player. While Refs. [11, 13] provide a clear explanation of the algorithm's basic structure (which is based on the *Metropolis algorithm*[22, 23]), we still need to figure out the game magnetization, entanglement susceptibility, correlation, player's payoff average, and payoff capacity for our particular scenario. So, this is a quick synopsis of the ABM algorithm:

1. At each site on the $1D$-IC, assign a random strategy to each player: *0* (strategy $\$_1$: say *defection*) or *1* (strategy $\$_2$: say *quantum*).

2. Choose a principal player at random to determine both its unique strategy as well as the strategy of its closest neighbour. The energy Δ of the principal player is ascertained based on the strategies that have been determined. The principal player's energy is computed for each of the two scenarios: either it chose the opposite strategy while preserving the closest neighbour's strategy, or it chose the same strategy as its closest neighbour.

3. For each of the two possible outcomes, the energy difference ($d\Delta$) is determined for the principal player. The current strategy of the principal player is flipped based on whether the Fermi function $(1+e^{\beta\cdot d\Delta})^{-1} > 0.5$; if not, it is not flipped. [22].

4. Now, based on the indicators, five distinct conditions emerge:

   - *Game magnetization*: After each run of the conditional spin-flipping loop, we calculate the difference between the number of players playing *quantum* (or, $\mathbb{Q}$) and the number of players playing *defect* (or, $\mathfrak{D}$). This gives the total magnetization $\tilde{\mu} = \sum_i \sigma_i$, for σ_i being the strategy (0 or 1) of the player at the i^{th}-site, for each cycle of the conditional loop. Finally, we take the average of the total magnetization for all the loops to determine the overall game magnetization, i.e., $\mu^{ABM} = \langle\tilde{\mu}\rangle$.

   - *Entanglement susceptibility*: Following Eqs. (21,23), the entanglement susceptibility can be determined from the variance of μ^{ABM} as, $\chi_\gamma^{ABM} = \frac{(\mathbb{B}+\mathbb{C})}{2}\sin(2\gamma)[\langle\tilde{\mu}^2\rangle - \langle\tilde{\mu}\rangle^2]$, where, $\tilde{\mu} = \sum_i \sigma_i$ and $\mu^{ABM} = \langle\tilde{\mu}\rangle$, respectively. Hence, following the previous steps for determining μ^{ABM}, we compute the μ^{ABM} variance and multiply the result by the factor: $\frac{1}{2}(\mathbb{B}+\mathbb{C})\sin(2\gamma)$, to get the entanglement susceptibility.

   - *Correlation*: We take into account two entangled principal player pairs, thus we slightly alter the first four steps to incorporate the needs of determining the correlation ($\mathfrak{c}_j^{ABM}$) between the two pairs of entangled players. Following the individual spin-flipping operations for the two randomly selected principal player pairs, the total correlation is increased by a correlation value of $+1$ if both players' strategies are the same and a correlation value of -1 if they are different.

   - *Player's payoff average*: Similar to the case of previous indicators, after all the spin-flipping operations, we determine the total energy of each individual Ising site, and the $-ve$ of this energy gives us the player's payoff average (or, $\langle\Lambda\rangle^{ABM}$).

   - *Payoff capacity*: Similar to χ_γ^{ABM}, the $\wp_C^{ABM}$ can be determined from the variance of average internal energy $\langle\mathbb{E}\rangle$, or, $-\langle\Lambda\rangle^{ABM}$ (see, Eqs. (28, 30) and Ref. [13]), and this gives us,

$$\wp_C^{ABM} = \frac{1}{2}[\langle\mathbb{E}^2\rangle - \langle\mathbb{E}\rangle^2]. \quad (30)$$

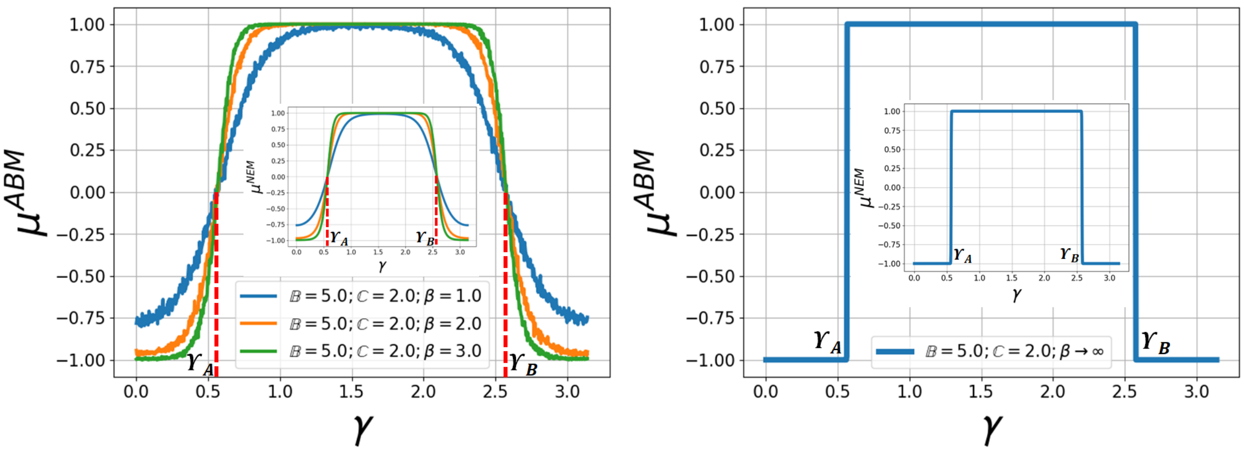

(a) $\mu^{ABM/NEM}$ vs γ

(b) $\mu^{ABM/NEM}$ vs γ in $\beta \to \infty$ (or, $T \to 0$) limit

FIG. 2: ABM and NEM (in *insets*): **Game magnetization** μ vs **entanglement** γ for **reward** $\mathbb{R} = (\mathbb{B} - \mathbb{C}) = 3.0$, **sucker's payoff** $\mathbb{S} = -\mathbb{C} = -2.0$, **temptation** $\mathbb{T} = \mathbb{B} = 5.0$, **punishment** $\mathbb{P} = 0.0$, $\gamma_A = 0.5639$ and $\gamma_B = 2.5777$ in QuPD.

Hence, following the previous steps for determining the player's payoff average, we calculate the variance of the internal energy (or, player's payoff average) and multiply it with the factor $\frac{1}{2}$ to get the payoff capacity.

5. Proceed to step 2 and carry out this procedure a *1000* times.

After reviewing the Python codes included in Appendices (A, B), one can have a better understanding of this algorithm. Given that our primary goal is to maximise the feasible payoff — which we can only do when our system reaches the energy equilibrium or the least energy configuration — we see that the likelihood of strategy switching drops as the energy difference $d\Delta$ increases.

III. RESULTS AND ANALYSIS

In our version of QuPD, there are effectively 2 game payoffs: Cooperation bonus ($\mathbb{B}$) and the Cost ($\mathbb{C}$), along with the measure of Entanglement (γ), with $\mathbb{B} \geq \mathbb{C} \geq 0$. We also restrict the value of $\gamma \in [0, \pi]$, respectively. When $\gamma = \frac{\pi}{2}$, we observe maximal entanglement among the players, and this signifies a *Bell state*. Here, we will analyze the variation of all five indicators: Game magnetization, Entanglement susceptibility, Correlation, Player's payoff average and Payoff capacity, with respect to the Entanglement γ while $\mathbb{B} = 5.0$ and $\mathbb{C} = 2.0$. One thing to note is that entanglement susceptibility, compared to game magnetization, is a far more accurate tool for gauging minute alterations in the number of players playing *defect* or *quantum*, owing to a change in entanglement γ.

A. Game magnetization (μ)

1. NEM

Using the given values of $\mathbb{B} = 5.0$, $\mathbb{C} = 2.0$ and the expression of μ^{NEM} in Eq. (22), we plot the variation of game magnetization with regard to changing values of γ, and they are given in the *insets* of Figs. 2a, 2b. We observe a change in the sign of the game magnetization from negative to positive and vice-versa at two particular values of γ. These indicate *first*-order phase transitions in the strategies adopted by the players, changing from *defect* to *quantum* and vice-versa, respectively. To determine the two critical values of γ (say, γ_A and γ_B) where these phase transitions occur, we equate $\mu^{NEM} = 0$ (see, Eq. (22)) and this leads to $\frac{(\mathbb{B}\sin^2\gamma - \mathbb{C}\cos^2\gamma)}{2} = 0$, finally giving us the relation between the critical γ values and the game payoffs $(\mathbb{B}, \mathbb{C})$ as: $\gamma_{A,B} = \tan^{-1}\sqrt{\mathbb{C}/\mathbb{B}}$. For $\mathbb{B} = 5.0$ and $\mathbb{C} = 2.0$, we have $\gamma = \tan^{-1}\sqrt{2/5} = 0.5639$ or 2.5777, i.e., $\gamma_A = 0.5639$ and $\gamma_B = 2.5777$, respectively (see, Figs. 2a, 2b) and they are independent of the *noise* β. Thus, the classical *defect* phase appears in the regime $\gamma \in [0, \gamma_A) \cup (\gamma_B, \pi]$ while the *quantum* phase appears in the regime $\gamma \in [\gamma_A, \gamma_B]$. For any general case, if $\mathbb{B} \gg \mathbb{C}$, then $\gamma_{A,B} = \tan^{-1}\sqrt{\mathbb{C}/\mathbb{B}} \to 0$ or π, and this indicates that the classical *defect* ($\mathfrak{D}$) phase disappears and the *quantum* phase is the only phase. By definition (see, CPD in Sec. II A), $\mathbb{B}$ is always greater than $\mathbb{C}$, hence, there always exists a quantum phase, otherwise, if $\mathbb{B} = \mathbb{C}$ or $\mathbb{B} < \mathbb{C}$, then the prisoner's dilemma disappears. However, when $\mathbb{B} \sim \mathbb{C}$, $\gamma_{A,B} = \tan^{-1}\sqrt{\mathbb{C}/\mathbb{B}} \approx \tan^{-1}(\pm 1) \to \frac{\pi}{4}$ or $\frac{3\pi}{4}$, indicating that the classical *defect* phase appears in the region $\gamma \in [0, \frac{\pi}{4}) \cup (\frac{3\pi}{4}, \pi]$ while the *quantum* phase appears in the region $\gamma \in [\frac{\pi}{4}, \frac{3\pi}{4}]$.

In the Z-N limit, i.e., $T \to 0$ (or, $\beta \to \infty$), if γ lies between γ_A and γ_B, then $\mu^{NEM} \to 1$, $\forall\ \gamma_A < \gamma < \gamma_B$, indicating that all players play the *quantum* strategy. However, when γ is either lower than γ_A or greater than γ_B, i.e., $\gamma \in [0, \gamma_A) \cup (\gamma_B, \pi]$, in the same Z-N limit, $\mu^{NEM} \to -1$, $\forall\ \gamma \in [0, \gamma_A) \cup (\gamma_B, \pi]$, indicating that all players play the *defect* strategy. In the I-N limit, i.e., $T \to \infty$ (or, $\beta \to 0$), $\mu^{NEM} \to 0$, implying that the players opt for their strategies randomly, resulting in an equiprobable number selecting *defect* and *quantum*, respectively.

2. ABM

For the given values of $\mathcal{T} = 0$ and $\mathcal{F} = \frac{(\mathbb{B}\sin^2\gamma - \mathbb{C}\cos^2\gamma)}{2}$ in Eq. (21), we have the Energy matrix $\Delta = -\Lambda$ (see, Eq. (12)). Thus,

$$\Delta = \begin{bmatrix} -(\mathbb{B}-\mathbb{C}) & -(\mathbb{B}\sin^2\gamma - \mathbb{C}\cos^2\gamma) \\ -(\mathbb{B}\cos^2\gamma - \mathbb{C}\sin^2\gamma) & 0 \end{bmatrix}. \tag{31}$$

Following the algorithm given in Sec. II B 2, for $\mathbb{B} = 5.0$ and $\mathbb{C} = 2.0$, we determine the ABM game magnetization (μ^{ABM}), and its variation with the entanglement γ is shown in Figs. 2a, 2b. We observe exactly the same results obtained via both NEM and ABM in the finite and limiting values of β. For $\beta > 0$, when $\gamma \in [0, \gamma_A) \cup (\gamma_B, \pi]$, the majority of players play *defect* over *quantum*. However, for the same $\beta > 0$, when $\gamma \in [\gamma_A, \gamma_B]$, the *quantum* phase appears, and a majority of players play *quantum*.

In the Z-N limit, i.e., $T \to 0$ (or, $\beta \to \infty$), $\mu^{ABM} \to 1$, $\forall\ \gamma \in [\gamma_A, \gamma_B]$, indicating that all players play the *quantum* strategy. However, when $\gamma \in [0, \gamma_A) \cup (\gamma_B, \pi]$, in the same Z-N limit, $\mu^{ABM} \to -1$, $\forall\ \gamma \in [0, \gamma_A) \cup (\gamma_B, \pi]$, indicating that all players play the *defect* strategy. In the I-N limit, i.e., $T \to \infty$ (or, $\beta \to 0$), $\mu^{ABM} \to 0$, implying that the players oft for their strategies randomly, resulting in an equiprobable number selecting *defect* and *quantum*, respectively.

3. Analysis of game magnetization

The analysis of game magnetization: μ^{NEM} as well as μ^{ABM}, will be done in this subsection. We observe in Fig. 2 that when $\gamma \to \frac{\pi}{2}$, i.e., *maximal entanglement*, $\mu^{ABM} = \mu^{NEM} \to 1$, indicating that all players play the *quantum* strategy. However, when $\gamma \to 0$ or π, i.e., *zero entanglement*, a large fraction of players play the classical *defect* strategy. For both finite and limiting β values, we observe *first*-order phase transitions at the two critical values of γ (i.e., at γ_A and γ_B) and the values of $\gamma_{A,B}$ depends on the payoffs $\mathbb{B}$ and $\mathbb{C}$ via the relation: $\gamma_{A,B} = \tan^{-1}\sqrt{\mathbb{C}/\mathbb{B}}$ (see, Sec. III A 2). For fixed values of γ (say, $\gamma = \frac{\pi}{6}$) and $\mathbb{C}$ (say, $\mathbb{C} = 2.0$), if we vary $\mathbb{B}$ from $\mathbb{B} \sim \mathbb{C}$ to $\mathbb{B} \gg \mathbb{C}$, while satisfying the criterion: $\mathbb{B} > \mathbb{C}$,

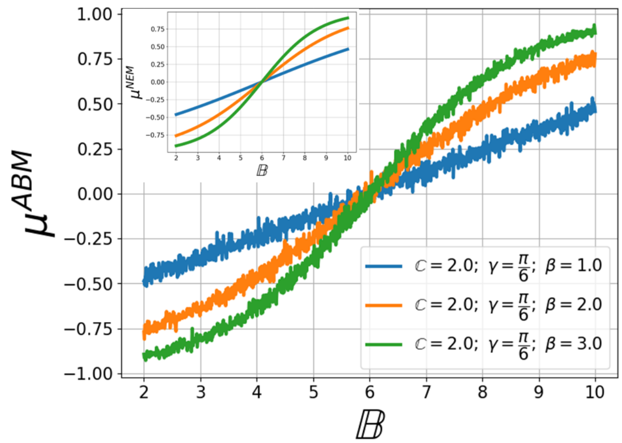

FIG. 3: ABM and NEM (in *insets*): $\mu^{ABM/NEM}$ vs changing **cooperation bonus** $\mathbb{B}$ for fixed **cost** $\mathbb{C} = 2.0$ and **entanglement** $\gamma = \frac{\pi}{6}$ in QuPD.

we observe a phase transition from *defect* to *quantum* as the cooperation bonus, i.e., $\mathbb{B}$ increases, and the phase transition (PT) occurs at: $\mathbb{B}_{PT} = \mathbb{C}\cot^2\gamma$ (see, Fig. 3). Similarly, for fixed γ and $\mathbb{B}$, if we vary $\mathbb{C}$ from $\mathbb{C} \ll \mathbb{B}$ to $\mathbb{C} \sim \mathbb{B}$, while satisfying the criterion: $\mathbb{C} < \mathbb{B}$, we observe a phase transition from *quantum* to *defect* as the cost associated with the game, i.e., $\mathbb{C}$ increases, and the phase transition occurs at: $\mathbb{C}_{PT} = \mathbb{B}\tan^2\gamma$. Hence, the game payoffs, i.e., $(\mathbb{B}, \mathbb{C})$ can also induce phase transition as seen from Fig. 3. Thus, we can have the phase transition(s) occurring in QuPD via both game payoffs and entanglement.

B. Entanglement susceptibility (χ_γ)

1. NEM

Using the given values of $\mathbb{B} = 5.0$, $\mathbb{C} = 2.0$ and the expression of χ_γ^{NEM} in Eq. (23), we plot the variation of entanglement susceptibility with regard to changing values of γ and they are shown in the *insets* of Figs. 4a, 4b. Here, in the $\beta \to \infty$ (i.e., Z-N) limit, we observe *two* sharp discontinuous peaks at two values of γ. To determine these critical γ values where $\chi_\gamma^{NEM} \to \infty$, in the $\beta \to \infty$ limit, we equate $\frac{1}{\chi_\gamma^{NEM}} \to 0$ (see, Eq. (23)) and we get the condition: $\mathcal{N} = \frac{1}{2}(\mathbb{B}\sin^2\gamma - \mathbb{C}\cos^2\gamma) = 0$, and this gives us the same expression for the critical γ's as in the case of game magnetization, i.e., $\gamma_{A,B} = \tan^{-1}\sqrt{\mathbb{C}/\mathbb{B}}$. For $\mathbb{B} = 5.0$ and $\mathbb{C} = 2.0$, we have $\gamma = \tan^{-1}\sqrt{2/5} = 0.5639$ or 2.5777. Therefore, we have $\gamma_A = 0.5639$ and $\gamma_B = 2.5777$, for the given values of $\mathbb{B} = 5.0$ and $\mathbb{C} = 2.0$ (see, Figs. 4a, 4b) and they are independent of the *noise* β.

When β is finite, as $\gamma \in [0, \gamma_A]$ gradually increases, we note that the strategy switching rate from *defect* to

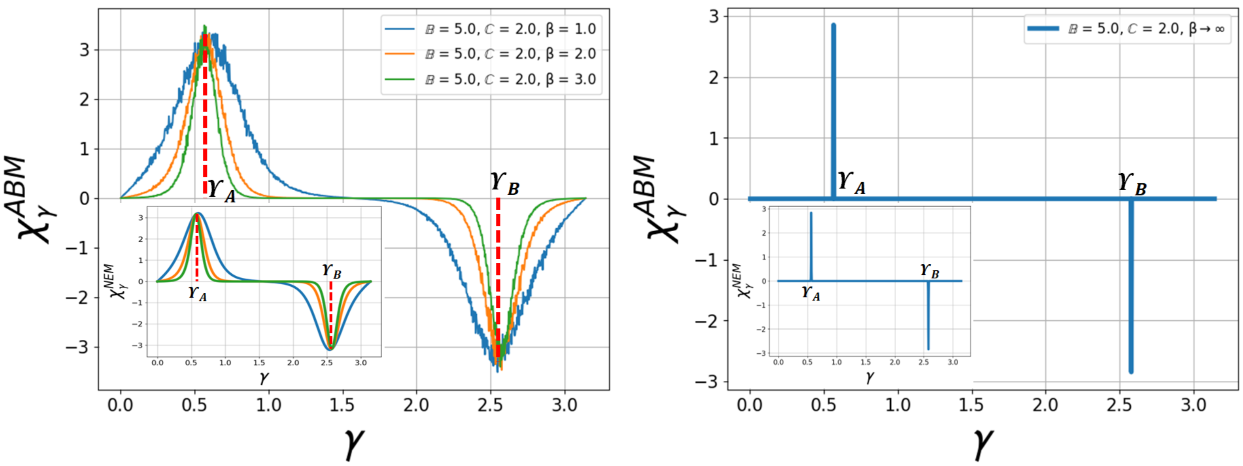

(a) $\chi_\gamma^{ABM/NEM}$ vs γ (b) $\chi_\gamma^{ABM/NEM}$ vs γ in $\beta \to \infty$ (or, $T \to 0$) limit

FIG. 4: ABM and NEM (in *insets*): **Entanglement susceptibility** χ_γ vs **entanglement** γ for **reward** $\mathbb{R} = (\mathbb{B} - \mathbb{C}) = 3.0$, **sucker's payoff** $\mathbb{S} = -\mathbb{C} = -2.0$, **temptation** $\mathbb{T} = \mathbb{B} = 5.0$, **punishment** $\mathbb{P} = 0.0$, $\gamma_A = 0.5639$ and $\gamma_B = 2.5777$ in QuPD.

quantum also increases, and this rate peaks at $\gamma = \gamma_A$. Then, as we increase the value of γ from γ_A to $\gamma = \frac{\pi}{2}$, the switching rate decreases, even though *quantum* strategy still remains the dominant strategy. At maximal entanglement, i.e., $\gamma = \frac{\pi}{2}$, the entanglement susceptibility vanishes since all the players play *quantum*, and they do not shift to *defect* on minute changes in γ. However, as we further increase the γ value from $\frac{\pi}{2}$ to γ_B, the strategy switching rate from *quantum* to *defect* increases, peaking at γ_B, and we observe that *defect* gradually becomes the dominant strategy of most players. For $\gamma = 0$ or π, a large fraction of players play *defect*. In the Z-N limit, i.e., $T \to 0$ (or, $\beta \to \infty$), $\chi_\gamma^{NEM} \to 0,\ \forall\ \gamma \neq \{\gamma_A, \gamma_B\}$ and here we observe the two sharp discontinuous peaks at $\gamma = \gamma_A$ and $\gamma = \gamma_B$ as discussed before. They indicate two *first*-order phase transitions at γ_A and γ_B since the game magnetization plot shows a discontinuity at γ_A and γ_B in the Z-N limit (see, Fig. 2b). The *first*-order phase transition is also a characteristic of *Type-I* superconductors (below a certain critical temperature and in the absence of an external field), and this shows that entanglement plays an important role in exhibiting phase transitions in quantum games like QuPD. In Z-N limit, for $\gamma \neq \{\gamma_A, \gamma_B\}$, the $\mu^{NEM} \to \pm 1$ and hence they do not change with a changing γ, resulting in $\chi_\gamma^{NEM} \to 0,\ \forall\ \gamma \neq \{\gamma_A, \gamma_B\}$.

In the I-N limit, i.e., $T \to \infty$ (or, $\beta \to 0$), $\chi_\gamma^{NEM} \to \frac{(\mathbb{B}+\mathbb{C})}{2} \sin(2\gamma),\ \forall\ \gamma$, implying that the players opt for their strategies randomly. The interesting part to discuss here is the unique expression of $\lim_{\beta\to 0} \chi_\gamma^{NEM} \to \frac{(\mathbb{B}+\mathbb{C})}{2} \sin(2\gamma),\ \forall\ \gamma$ in the I-N limit. In the I-N limit, Taylor expanding the expression of μ^{NEM}, in Eq. (22), around β, makes this very easily verifiable, where the 1^{st}-order correction (say, $\mu^{(1)}$) of μ^{NEM}, is given as, $\mu^{(1)} = -\frac{\beta(\mathbb{B}+\mathbb{C})}{4} \cos(2\gamma)$, leading to the 0^{th}-order χ_γ^{NEM} correction as,

$$\lim_{\beta\to 0} \chi_\gamma^{(0)} = \lim_{\beta\to 0} \frac{1}{\beta} \frac{\partial}{\partial\gamma} \mu^{(1)} = \frac{(\mathbb{B}+\mathbb{C})}{2} \sin(2\gamma). \qquad (32)$$

The *higher* order expansion terms of χ_γ^{NEM} about β, in the I-N limit, vanishes. This explains why we get a non-zero expression for χ_γ in the I-N limit.

2. ABM

For the given values of $\mathcal{T} = 0$ and $\mathcal{F} = \frac{(\mathbb{B}\sin^2\gamma - \mathbb{C}\cos^2\gamma)}{2}$ in Eq. (21), we have $\Delta = -\Lambda$ (see, Eq. (12)). Thus,

$$\Delta = \begin{bmatrix} -(\mathbb{B}-\mathbb{C}) & -(\mathbb{B}\sin^2\gamma - \mathbb{C}\cos^2\gamma) \\ -(\mathbb{B}\cos^2\gamma - \mathbb{C}\sin^2\gamma) & 0 \end{bmatrix}. \qquad (33)$$

Following the algorithm given in Sec. II B 2, for $\mathbb{B} = 5.0$ and $\mathbb{C} = 2.0$, we determine the ABM entanglement susceptibility (χ_γ^{ABM}), and its variation with the entanglement γ is shown in Figs. 4a, 4b. Here also, we observe exactly the same results as obtained for entanglement susceptibility, via NEM, in the finite and limiting values of β. For finite β and increasing values of $\gamma \in [0, \gamma_A]$, we note that the strategy switching rate from *defect* to *quantum* also increases, reaching the peak value at $\gamma = \gamma_A$. On further increase of γ value, from γ_A to $\gamma = \frac{\pi}{2}$, the switching rate decreases, even though *quantum* still remains the dominant strategy. In the case of maximal entanglement, i.e., $\gamma = \frac{\pi}{2}$, χ_γ^{ABM} vanishes since all the players play the *quantum* strategy, and they do not change their strategies on minute changes in γ. On further increase of γ value, from $\frac{\pi}{2}$ to γ_B, the strategy switching rate from *quantum*

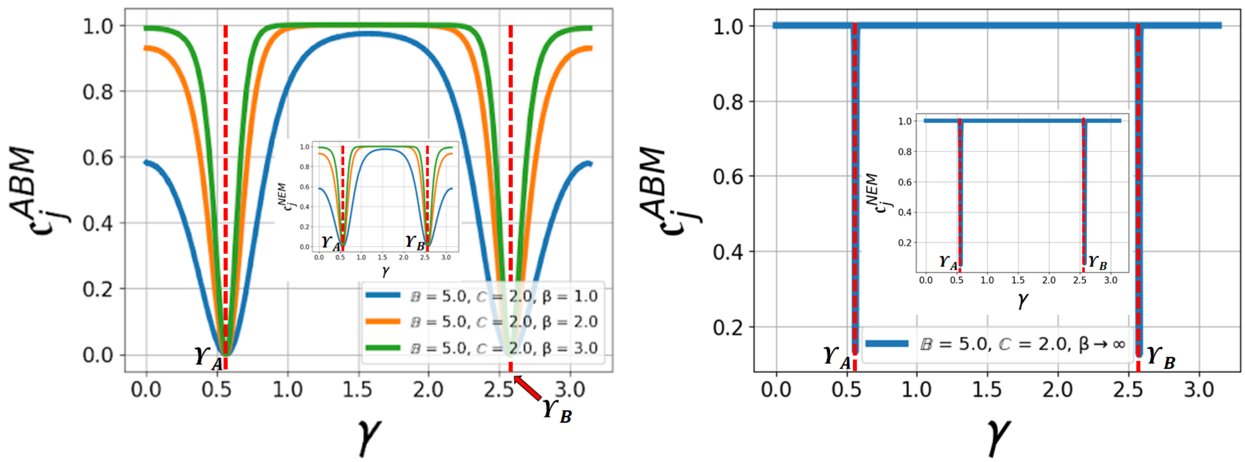

(a) $\mathfrak{c}_j^{ABM/NEM}$ vs γ

(b) $\mathfrak{c}_j^{ABM/NEM}$ vs γ in $\beta \to \infty$ (or, $T \to 0$) limit

FIG. 5: ABM and NEM (in *insets*): **Correlation** $\mathfrak{c}_j$ vs γ for **distance** $j = 11$, **reward** $\mathbb{R} = (\mathbb{B} - \mathbb{C}) = 3.0$, **sucker's payoff** $\mathbb{S} = -\mathbb{C} = -2.0$, **temptation** $\mathbb{T} = \mathbb{B} = 5.0$, **punishment** $\mathbb{P} = 0.0$, $\gamma_A = 0.5639$ and $\gamma_B = 2.5777$ in QuPD.

to *defect* increases, peaking at γ_B, and we observe that *defect* gradually becomes the dominant strategy of most players. For $\gamma = 0$ or π, a large fraction of players play *defect*.

In the Z-N limit, i.e., $T \to 0$ (or, $\beta \to \infty$), $\chi_\gamma^{ABM} \to 0, \ \forall\ \gamma \neq \{\gamma_A, \gamma_B\}$. Here also, we observe two sharp discontinuous peaks, at $\gamma = \gamma_A$ and $\gamma = \gamma_B$, indicating the two *first*-order phase transitions at γ_A and γ_B. As seen in Fig. 2b, the game magnetization plot shows a discontinuity at γ_A and γ_B in the Z-N limit. In Z-N limit, for $\gamma \neq \{\gamma_A, \gamma_B\}$, the $\mu^{ABM} \to \pm 1$ and hence they do not change with a changing γ, resulting in $\chi_\gamma^{ABM} \to 0, \ \forall\ \gamma \neq \{\gamma_A, \gamma_B\}$. In the I-N limit, i.e., $T \to \infty$ (or, $\beta \to 0$), $\chi_\gamma^{ABM} \to \frac{(\mathbb{B}+\mathbb{C})}{2} \sin(2\gamma), \ \forall\ \gamma$, implying that the players opt for their strategies randomly. In the I-N limit, even though $\langle \mu^{ABM} \rangle \to 0$ due to strategy selection randomization, $\langle (\mu^{ABM})^2 \rangle \to 1$ and this gives us the value of $\chi_\gamma^{ABM} = \frac{(\mathbb{B}+\mathbb{C})}{2} \sin(2\gamma)$ (see, Eq. (23)) in the $\beta \to 0$ (or, I-N) limit.

3. Analysis of entanglement susceptibility

The analysis of entanglement susceptibility: χ_γ^{NEM} as well as χ_γ^{ABM}, will be done in this subsection. From Fig. 4, we observe that for all $\gamma \to \{0, \frac{\pi}{2}, \pi\}$, i.e., for both *minimal* (i.e., $\gamma \to 0$ or π) and *maximal entanglement* (i.e., $\gamma \to \frac{\pi}{2}$), $\chi_\gamma^{ABM} = \chi_\gamma^{NEM} \to 0$, indicating that there is no phase transition among the players. This can also be verified from the game magnetization result (see, Fig. 2) where we observe that for *finite* as well as *limiting* values of β, when $\gamma \to \{0, \frac{\pi}{2}, \pi\}$, a large fraction of players play either *defect* (for $\gamma \to 0$ or π) or *quantum* (for $\gamma \to \frac{\pi}{2}$), and this leads to a vanishing χ_γ. Interestingly, in the Z-N (or, $\beta \to \infty$) limit, we observe two *first*-order phase transitions, as shown in Fig. 4b, at the two critical values of γ (i.e., at γ_A and γ_B). The values of $\gamma_{A,B}$, where we observe the phase transitions, depend on the payoffs $\mathbb{B}$ and $\mathbb{C}$ via the relation: $\gamma_{A,B} = \tan^{-1}\sqrt{\mathbb{C}/\mathbb{B}}$ (see, Sec. III A 2). The two *first*-order phase transition points, i.e., γ_A and γ_B, depend on both game payoffs (i.e., $\mathbb{B}$, $\mathbb{C}$), indicating that the game payoffs can also induce phase transition as seen in the case of μ.

C. Correlation ($\mathfrak{c}_j$)

1. NEM

Using the given values of $\mathbb{B} = 5.0$, $\mathbb{C} = 2.0$ and the expression of $\mathfrak{c}_j^{NEM}$ in Eqs. (25, 26, 27), we plot the variation of correlation with regard to changing values of γ and they are shown in the *insets* of Figs. 5a, 5b. In both Figs. 5a and 5b, we observe a vanishing correlation at two particular values of γ, and this signifies a *first*-order phase transition. For $\mathfrak{c}_j^{NEM} \to 0$, using Eqs. (25, 26, 27), we get the condition: $\sinh^2 \beta\mathcal{N} = 0$, i.e., $\mathcal{N} = \frac{1}{2}(\mathbb{B}\sin^2\gamma - \mathbb{C}\cos^2\gamma) = 0$, and this gives us the same expression for the critical γ's as before, i.e., $\gamma_{A,B} = \tan^{-1}\sqrt{\mathbb{C}/\mathbb{B}}$. For $\mathbb{B} = 5.0$ and $\mathbb{C} = 2.0$, we have $\gamma = \tan^{-1}\sqrt{2/5} = 0.5639$ or 2.5777. Therefore, we have $\gamma_A = 0.5639$ and $\gamma_B = 2.5777$ for the given values of $\mathbb{B} = 5.0$ and $\mathbb{C} = 2.0$ (see, Figs. 5a, 5b) and they are independent of the *noise* β.

When β is finite, as $\gamma \in [0, \gamma_A]$ gradually increases, we find an initial drop in the strategy correlation, reaching a minimum at $\gamma = \gamma_A$. This is mainly attributed to the fact that while $\gamma \to \gamma_1$, the players tend to shift from classical *defect* to *quantum*, resulting in a lowering of correlation among the players. Then, as we increase the value of γ from γ_A to $\gamma = \frac{\pi}{2}$, the correlation increases since most of the players now play *quantum* as $\gamma \to \frac{\pi}{2}$. At maximal entanglement, i.e., $\gamma = \frac{\pi}{2}$, the correlation is maximum since, in this case, all the players play *quantum*, and they do not shift to *defect* on minute changes in γ. However, as we further increase the γ value from $\frac{\pi}{2}$ to γ_B, the strategy correlation again decreases due to a strategy shift from *quantum* to *defect* among the players, reaching a minimum at γ_B. When $\gamma > \gamma_B$, the majority of players switch to *defect*, thus increasing the correlation. When $\gamma = 0$ or π, a large fraction of players play *defect*. In the Z-N limit, i.e., $T \to 0$ (or, $\beta \to \infty$), $\mathfrak{c}_j^{NEM} \to 1,\ \forall\ \gamma \neq \{\gamma_A, \gamma_B\}$. Here, we also observe two sharp discontinuous phase transition peaks, at γ_A and γ_B (see, Fig. 5b), when all players shift from *defect* to *quantum* (at $\gamma = \gamma_A$) and back to *defect* (at $\gamma = \gamma_B$) as the γ value increases from 0 to π. In the I-N limit, i.e., $T \to \infty$ (or, $\beta \to 0$), $\mathfrak{c}_j^{NEM} \to 0,\ \forall\ \gamma$, implying that the players opt for their strategies randomly, resulting in vanishing correlation.

2. ABM

For the given values of $\mathcal{T} = 0$ and $\mathcal{F} = \frac{(\mathbb{B}\sin^2\gamma - \mathbb{C}\cos^2\gamma)}{2}$ in Eq. (21), we have the Energy matrix $\Delta = -\Lambda$ (see, Eq. (12)). Thus,

$$\Delta = \begin{bmatrix} -(\mathbb{B} - \mathbb{C}) & -(\mathbb{B}\sin^2\gamma - \mathbb{C}\cos^2\gamma) \\ -(\mathbb{B}\cos^2\gamma - \mathbb{C}\sin^2\gamma) & 0 \end{bmatrix}. \tag{34}$$

Following the algorithm given in Sec. II B 2, for $\mathbb{B} = 5.0$ and $\mathbb{C} = 2.0$, we determine the ABM correlation ($\mathfrak{c}_j^{ABM}$), and its variation with the entanglement γ is shown in Figs. 5a, 5b. We again observe exactly the same results as obtained for correlation, via NEM, in the finite and limiting values of β. When β is finite, as $\gamma \in [0, \gamma_A]$ gradually increases, we find an initial drop in the strategy correlation, reaching a minimum at $\gamma = \gamma_A$. Then, as we increase the value of γ from γ_A to $\gamma = \frac{\pi}{2}$, the correlation increases. At maximal entanglement, i.e., $\gamma = \frac{\pi}{2}$, the correlation is maximum. As we further increase the γ value from $\frac{\pi}{2}$ to γ_B, the correlation again decreases, reaching a minimum at γ_B.

In the Z-N limit, i.e., $T \to 0$ (or, $\beta \to \infty$), $\mathfrak{c}_j^{ABM} \to 1,\ \forall\ \gamma \neq \{\gamma_A, \gamma_B\}$. As shown in Fig. 5b, we observe two sharp phase transition peaks, at γ_A and γ_B, when all players shift from *defect* to *quantum* (at $\gamma = \gamma_A$) and back to *defect* (at $\gamma = \gamma_B$) as the γ value increases from 0 to π. In the I-N limit, i.e., $T \to \infty$ (or, $\beta \to 0$), $\mathfrak{c}_j^{ABM} \to 0,\ \forall\ \gamma$, implying that the players opt for their strategies randomly, resulting in vanishing correlation.

3. Analysis of correlation

The analysis of correlation: $\mathfrak{c}_j^{NEM}$ as well as $\mathfrak{c}_j^{ABM}$, will be done in this subsection. From Fig. 5 we observe that for increasing values of β, for both *minimal* (i.e., $\gamma \to 0$ or π) and *maximal entanglement* (i.e., $\gamma \to \frac{\pi}{2}$), $c_j^{ABM} = \mathfrak{c}_j^{NEM} \to 1$, indicating maximum correlation among the strategies adopted by the players. In both $\gamma \to 0$ and $\gamma \to \pi$ limits, for increasing β, a large fraction of players play the *defect* strategy, leading to maximum correlation. Similarly, in the $\gamma \to \frac{\pi}{2}$ limit, almost all players adopt the *quantum* strategy, and this also leads to a maximum correlation. In the Z-N (or, $\beta \to \infty$) limit, we observe two *first*-order phase transition peaks, as shown in Fig. 5b, at the two critical values of γ (i.e., at γ_A and γ_B). The values of $\gamma_{A,B}$, where we observe the phase transitions, depend on the payoffs $\mathbb{B}$ and $\mathbb{C}$ via the relation: $\gamma_{A,B} = \tan^{-1}\sqrt{\mathbb{C}/\mathbb{B}}$, and both $\mathbb{B}$ as well as $\mathbb{C}$ can also induce phase transition(s) in a similar way to what we discussed in the case of game magnetization μ.

D. Player's payoff average ($\langle\Lambda\rangle$)

1. NEM

Using the given values of $\mathbb{B} = 5.0$, $\mathbb{C} = 2.0$ and the expression of $\langle\Lambda\rangle^{NEM}$ in Eq. (28), we plot the variation of $\langle\Lambda\rangle^{NEM}$ with regard to changing values of γ and they are given in the *insets* of Figs. 6a, 6b. In both Figs. 6a and 6b, we observe a vanishing payoff average at two particular values of γ, signifying a *first*-order phase transition. For $\langle\Lambda\rangle^{NEM} \to 0$, using Eq. (28), we get the condition: $\mathcal{N} = \frac{1}{2}(\mathbb{B}\sin^2\gamma - \mathbb{C}\cos^2\gamma) = 0$, and this gives us the same expression for the critical γ's as seen for the previous indicators, i.e., $\gamma_{A,B} = \tan^{-1}\sqrt{\mathbb{C}/\mathbb{B}}$. For $\mathbb{B} = 5.0$ and $\mathbb{C} = 2.0$, we have $\gamma = \tan^{-1}\sqrt{2/5} = 0.5639$ or 2.5777. Therefore, we have $\gamma_A = 0.5639$ and $\gamma_B = 2.5777$ for given values of $\mathbb{B} = 5.0$ and $\mathbb{C} = 2.0$ (see, Figs. 6a, 6b) and they are independent of the *noise* β.

When β is finite, as $\gamma \in [0, \gamma_A]$ gradually increases, we find an initial drop in the $\langle\Lambda\rangle^{NEM}$ value, reaching a minimum at $\gamma = \gamma_A$. This is mainly attributed to the fact that while γ approaches γ_1, the players tend to switch from classical *defect* to *quantum*, resulting in a lowering of feasible payoffs accessible to all players, see the payoff matrix given in Eq. (12) for the payoffs associated with $[\mathbb{Q}, \mathfrak{D}]$ or $[\mathfrak{D}, \mathbb{Q}]$ case. Then, as we increase the value of γ from γ_A to $\gamma = \frac{\pi}{2}$, $\langle\Lambda\rangle^{NEM}$ increases since most of the players have switched to *quantum* as γ approaches $\frac{\pi}{2}$, resulting in a comparatively better average payoff than the classical strategy (*defect*) payoffs (see, $[\mathbb{Q}, \mathbb{Q}]$-payoff in Eq. (12)). At maximal entanglement, i.e., $\gamma = \frac{\pi}{2}$, $\langle\Lambda\rangle^{NEM}$ is maximum since, in this case, all the players play *quantum* and they do not shift to *defect* on minute changes in γ, resulting in the best possible payoff available to each player. However, as we further increase the γ value from $\frac{\pi}{2}$ to γ_B, $\langle\Lambda\rangle^{NEM}$ again decreases due to a switch from *quantum* to *defect* among the players, reaching a minimum at γ_B. When $\gamma > \gamma_B$, the majority of players switch over to *defect*, thus increasing the classical

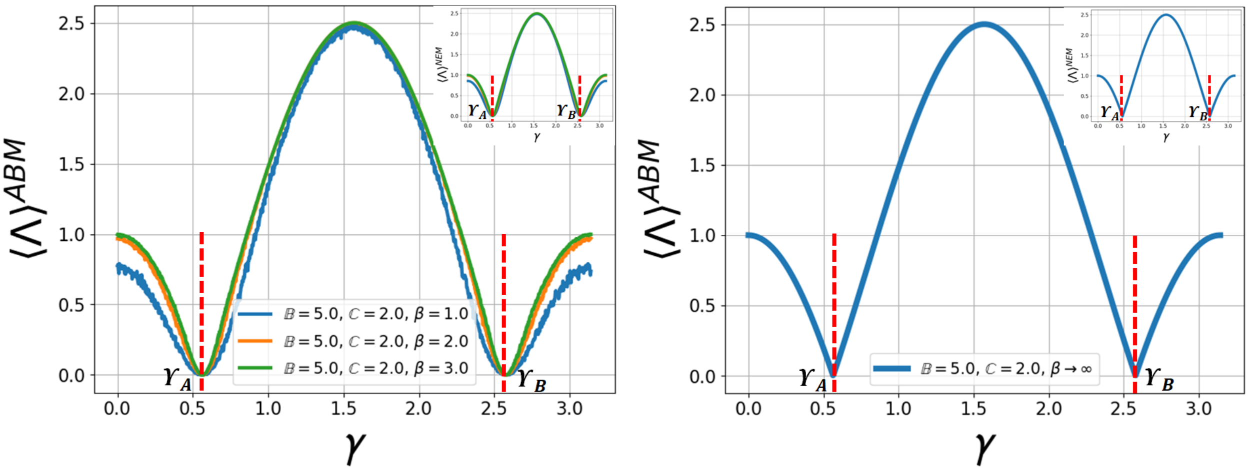

(a) $\langle\Lambda\rangle^{ABM/NEM}$ vs γ

(b) $\langle\Lambda\rangle^{ABM/NEM}$ vs γ in $\beta\to\infty$ (or, $T\to 0$) limit

FIG. 6: ABM and NEM (in *insets*): **Player's payoff average** $\langle\Lambda\rangle$ vs γ for **reward** $\mathbb{R}=(\mathbb{B}-\mathbb{C})=3.0$, **sucker's payoff** $\mathbb{S}=-\mathbb{C}=-2.0$, **temptation** $\mathbb{T}=\mathbb{B}=5.0$, **punishment** $\mathbb{P}=0.0$, $\gamma_A=0.5639$ and $\gamma_B=2.5777$ in QuPD.

average payoff associated with the *defect* strategy. When $\gamma=0$ or π, a large fraction of players play *defect*.

In the Z-N limit, i.e., $T\to 0$ (or, $\beta\to\infty$), $\langle\Lambda\rangle^{NEM}\to\frac{|\mathbb{B}\sin^2\gamma-\mathbb{C}\cos^2\gamma|}{2}$, $\forall\,\gamma$. This shows that the player's payoff average depends on the entanglement γ and always satisfies $\langle\Lambda\rangle^{NEM}\geq 0$, irrespective of the payoffs. In the I-N limit, i.e., $T\to\infty$ (or, $\beta\to 0$), $\langle\Lambda\rangle^{NEM}\to 0$, $\forall\,\gamma$, implying that the players opt for their strategies randomly, leading to payoff randomization. By summing up the four payoffs (or, the matrix elements) given in the energy (or, $-ve$ payoff) matrix in Eq. (36), we indeed get a vanishing average payoff per player.

2. ABM

To determine the individual player's payoff average, we start with the given values of $\mathcal{T}=0$ and $\mathcal{F}=\frac{(\mathbb{B}\sin^2\gamma-\mathbb{C}\cos^2\gamma)}{2}$ in Eq. (21), respectively. The Energy matrix $\Delta=-\Lambda$ (see, Eq. (12)) is again given as,

$$\Delta=\begin{bmatrix}-(\mathbb{B}-\mathbb{C}) & -(\mathbb{B}\sin^2\gamma-\mathbb{C}\cos^2\gamma)\\ -(\mathbb{B}\cos^2\gamma-\mathbb{C}\sin^2\gamma) & 0\end{bmatrix}. \tag{35}$$

However, this time, instead of considering the Δ in Eq. (35), we consider a modified Δ (say, Δ')[13] whose elements are the linear transformations of the original energy matrix elements given in Eq. (35) (see, the set of linear transformations given in Eq. (17)). Both these matrices have a one-to-one correspondence, and hence, the Nash equilibrium is preserved. So, we redefine the energy matrix as,

$$\Delta'=\begin{bmatrix}-\frac{(\mathbb{B}\sin^2\gamma-\mathbb{C}\cos^2\gamma)}{2} & -\frac{(\mathbb{B}\sin^2\gamma-\mathbb{C}\cos^2\gamma)}{2}\\ \frac{(\mathbb{B}\sin^2\gamma-\mathbb{C}\cos^2\gamma)}{2} & \frac{(\mathbb{B}\sin^2\gamma-\mathbb{C}\cos^2\gamma)}{2}\end{bmatrix}. \tag{36}$$

Both Δ in Eq. (35) and Δ' in Eq. (36) are equivalent to each other. Now, by following the algorithm given in Sec. II B 2, for $\mathbb{B}=5.0$ and $\mathbb{C}=2.0$, we determine the ABM player's payoff average ($\langle\Lambda\rangle^{ABM}$), and its variation with the entanglement γ is shown in Figs. 6a, 6b. We again observe exactly the same results as obtained for $\langle\Lambda\rangle$, via NEM, in the finite and limiting values of β.

When β is finite, as $\gamma\in[0,\gamma_A]$ gradually increases, we find an initial drop in the $\langle\Lambda\rangle^{ABM}$ value, reaching a minimum at $\gamma=\gamma_A$. Then, as we increase the value of γ from γ_A to $\gamma=\frac{\pi}{2}$, $\langle\Lambda\rangle^{ABM}$ increases since most of the players switch to *quantum* as γ approaches $\frac{\pi}{2}$. At maximal entanglement, i.e., $\gamma=\frac{\pi}{2}$, $\langle\Lambda\rangle^{ABM}$ is maximum since, in this case, all the players play *quantum*, and they do not shift to *defect* on minute changes in γ. However, as we further increase the γ value from $\frac{\pi}{2}$ to γ_B, $\langle\Lambda\rangle^{ABM}$ again decreases due to a strategy shift from *quantum* to *defect* among the players, reaching a minimum at γ_B. When $\gamma>\gamma_B$, the majority of players choose to switch over to *defect*. In the Z-N limit, i.e., $T\to 0$ (or, $\beta\to\infty$), $\langle\Lambda\rangle^{ABM}\to\frac{|\mathbb{B}\sin^2\gamma-\mathbb{C}\cos^2\gamma|}{2}$, $\forall\,\gamma$. This shows that the player's payoff average, similar to what we observed in ABM, depends on the entanglement γ and always satisfies $\langle\Lambda\rangle^{ABM}\geq 0$, irrespective of the payoffs. In the I-N limit, i.e., $T\to\infty$ (or, $\beta\to 0$), $\langle\Lambda\rangle^{ABM}\to 0$, $\forall\,\gamma$, implying that the players opt for their strategies randomly, leading to payoff randomization.

3. Analysis of Player's payoff average

The analysis of the Player's payoff average: $\langle\Lambda\rangle^{NEM}$ as well as $\langle\Lambda\rangle^{ABM}$, will be done in this subsection. From Fig. 6, we observe that for increasing values of β, in *minimal entanglement* (i.e., $\gamma\to 0$ or π), $\langle\Lambda\rangle^{ABM}=$

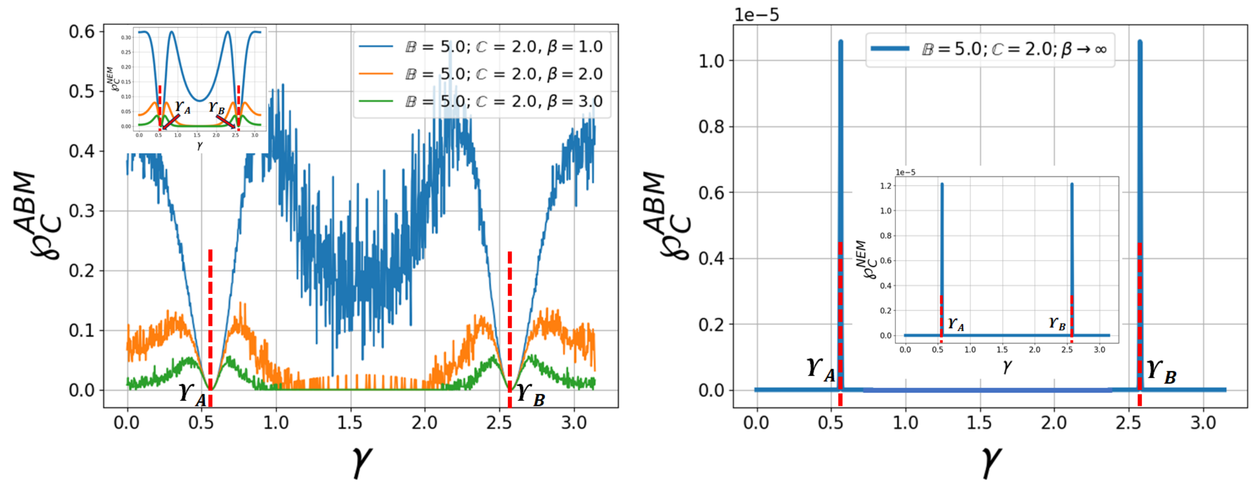

(a) $\wp_C^{ABM/NEM}$ vs γ

(b) $\wp_C^{ABM/NEM}$ vs γ in $\beta \to \infty$ (or, $T \to 0$) limit

FIG. 7: ABM and NEM (in *insets*): **Payoff capacity** $\wp_C$ vs **entanglement** γ for **reward** $\mathbb{R} = 3.0$, **sucker's payoff** $\mathbb{S} = 0.0$, **temptation** $\mathbb{T} = 5.0$, **punishment** $\mathbb{P} = 1.0$, $\gamma_A = 0.5639$ and $\gamma_B = 2.5777$ in QuPD.

$\langle\Lambda\rangle^{NEM} \to \frac{\mathbb{C}}{2} = 1$, for given $\mathbb{C} = 2.0$, indicating the average payoff associated with the classical *defect* ($\mathfrak{D}$) strategy, which in fact is the dominant strategy in this case. Meanwhile, in *maximal entanglement* (i.e., $\gamma \to \frac{\pi}{2}$), when all players play *quantum*, $\langle\Lambda\rangle^{ABM} = \langle\Lambda\rangle^{NEM} \to \frac{\mathbb{B}}{2} = \frac{5}{2}$, for given $\mathbb{B} = 5.0$, indicating the average payoff associated with the *quantum* ($\mathbb{Q}$) strategy. For any $(\mathbb{B}, \mathbb{C})$ that satisfies the criteria: $\mathbb{B} > \mathbb{C} > 0$, the average payoff associated with the *quantum* strategy always exceeds the average payoff associated with the *defect* strategy and this results in a large fraction of players switching their strategies from $\mathfrak{D} \to \mathbb{Q}$ when the entanglement $\gamma \in [\gamma_A, \gamma_B]$. For finite as well as limiting values of β, we observe a vanishing average payoff at both the critical γ points, i.e., γ_A and γ_B, and this signifies the change in phases from *defect* to *quantum* and vice-versa at γ_A and γ_B, respectively. Here too, the values of $\gamma_{A,B}$, where we observe the phase transitions, depend on the payoffs $\mathbb{B}$ and $\mathbb{C}$ via the relation: $\gamma_{A,B} = \tan^{-1}\sqrt{\mathbb{C}/\mathbb{B}}$, and both $\mathbb{B}$ as well as $\mathbb{C}$ can induce phase transition(s).

E. Payoff capacity ($\wp_C$)

1. NEM

Using the given values of $\mathbb{B} = 5.0$, $\mathbb{C} = 2.0$ and the expression of $\wp_C^{NEM}$ in Eq. (29), we plot the variation of $\wp_C^{NEM}$ with regard to changing values of γ and they are shown in the *insets* of Figs. 7a, 7b. In the $\beta \to \infty$ (i.e., Z-N) limit, we observe *two* sharp discontinuous peaks at two values of $\wp_C^{NEM}$, indicating *first*-order phase transitions. To determine these critical γ values where $\wp_C^{NEM} \to \infty$, in the $\beta \to \infty$ limit, we equate $\frac{1}{\wp_C^{NEM}} \to 0$ (see, Eq. (29)) and we again get the condition: $\frac{1}{2}(\mathbb{B}\sin^2\gamma - \mathbb{C}\cos^2\gamma) = 0$, and this gives us the same expression for the critical γ's, i.e., $\gamma_{A,B} = \tan^{-1}\sqrt{\mathbb{C}/\mathbb{B}}$. For $\mathbb{B} = 5.0$ and $\mathbb{C} = 2.0$, we have $\gamma = \tan^{-1}\sqrt{2/5} = 0.5639$ or 2.5777. Therefore, we have $\gamma_A = 0.5639$ and $\gamma_B = 2.5777$ for the given values of $\mathbb{B} = 5.0$, $\mathbb{C} = 2.0$ (see, Figs. 7a, 7b) and they are independent of the *noise* β.

When β is finite, as $\gamma \in [0, \gamma_A]$ gradually increases, we find an initial drop in the $\wp_C^{NEM}$ value, reaching a minimum at $\gamma = \gamma_A$. This is mainly attributed to the fact that while γ approaches γ_1, the players tend to switch from *defect* to *quantum*, resulting in a lowering of the average feasible payoffs accessible to the players, which further leads to a minimal change in the average payoff when there is a unit change in the *noise*. Then, as we increase the value of γ from γ_A to $\gamma = \frac{\pi}{2}$, $\wp_C^{NEM}$ first increases and then again it decreases since within this range of γ, the players update their strategies from *defect* to *quantum*, and hence we initially observe a significant alteration in the payoff owing to a unit change in the noise. However, when all players play *quantum*, then the payoffs do not change significantly with regards to a unit change in noise, resulting in a decrease of $\wp_C^{NEM}$ as γ approaches $\frac{\pi}{2}$. However, as we further increase the γ value from $\frac{\pi}{2}$ to γ_B, $\wp_C^{NEM}$ value again initially increases and then decreases due to the same logic as mentioned before, but now the strategy shift gets reversed, and the players tend to shift from *quantum* to *defect*. When $\gamma = 0$ or π, a large fraction of players play *defect*.

In the Z-N limit, i.e., $T \to 0$ (or, $\beta \to \infty$), $\wp_C^{NEM} \to 0$, $\forall\, \gamma \neq \{\gamma_A, \gamma_B\}$, indicating two phase transition peaks at γ_A and γ_B. In the Z-N limit, we see no variation in a player's payoff (i.e., the payoff becomes *constant*), which leads to a vanishing payoff capacity except at the two critical values of γ_A and γ_B, where we get vanishing

For QuPD game		**ABM**	**NEM**
μ	$\beta \to 0$	$0,\ \forall\ \gamma$	$0,\ \forall\ \gamma$
	$\beta \to \infty$	$+1,\ \forall\ \gamma_A < \gamma < \gamma_B$ $-1,\ \forall\ \gamma < \gamma_A$ or $\gamma > \gamma_B$	$+1,\ \forall\ \gamma_A < \gamma < \gamma_B$ $-1,\ \forall\ \gamma < \gamma_A$ or $\gamma > \gamma_B$
χ_γ	$\beta \to 0$	$\frac{(\mathbb{B}+\mathbb{C})}{2}\sin(2\gamma), \forall\ \gamma$	$\frac{(\mathbb{B}+\mathbb{C})}{2}\sin(2\gamma), \forall\ \gamma$
	$\beta \to \infty$	$0,\ \forall\ \gamma \neq \{\gamma_A, \gamma_B\}$	$0,\ \forall\ \gamma \neq \{\gamma_A, \gamma_B\}$
$\mathfrak{c}_{\mathbf{j}}$	$\beta \to 0$	$0,\ \forall\ \gamma$	$0,\ \forall\ \gamma$
	$\beta \to \infty$	$1,\ \forall\ \gamma \neq \{\gamma_A, \gamma_B\}$	$1,\ \forall\ \gamma \neq \{\gamma_A, \gamma_B\}$
$\mathbf{\Lambda}$	$\beta \to 0$	$0,\ \forall\ \gamma$	$0,\ \forall\ \gamma$
	$\beta \to \infty$	$\frac{\lvert\mathbb{B}\sin^2\gamma - \mathbb{C}\cos^2\gamma\rvert}{2},\ \forall\ \gamma$	$\frac{\lvert\mathbb{B}\sin^2\gamma - \mathbb{C}\cos^2\gamma\rvert}{2},\ \forall\ \gamma$
$\wp_{\mathbf{c}}$	$\beta \to 0$	$\frac{(\mathbb{B}\sin^2\gamma - \mathbb{C}\cos^2\gamma)^2}{3},\ \forall\ \gamma$	$\frac{(\mathbb{B}\sin^2\gamma - \mathbb{C}\cos^2\gamma)^2}{3},\ \forall\ \gamma$
	$\beta \to \infty$	$0,\ \forall\ \gamma \neq \{\gamma_A, \gamma_B\}$	$0,\ \forall\ \gamma \neq \{\gamma_A, \gamma_B\}$

TABLE I: QuPD game with reward $\mathbb{R} = (\mathbb{B} - \mathbb{C}) = 3.0$, **sucker's payoff** $\mathbb{S} = -\mathbb{C} = -2.0$, **temptation** $\mathbb{T} = \mathbb{B} = 5.0$, **punishment** $\mathbb{P} = 0.0$, inter-site distance j, $\gamma_A = 0.5639$, $\gamma_B = 2.5777$ and measure of noise β.

payoffs (see, Sec. III D 3) and this indicates the change in phases, i.e., from $\mathfrak{D} \to \mathbb{Q}$ and vice-versa, resulting in a small yet noticeable peak in the payoff capacity plot (see, Fig. 7b). In the I-N limit, i.e., $T \to \infty$ (or, $\beta \to 0$), $\wp_C^{NEM} \to \frac{(\mathbb{B}\sin^2\gamma - \mathbb{C}\cos^2\gamma)^2}{3}$, $\forall\ \gamma$, implying that the players opt for their strategies randomly. For finite non-zero β, $\wp_C^{NEM}$ is always $+ve$, indicating that $\langle\Lambda\rangle^{NEM}$ changes at a faster rate with increasing *noise*.

2. ABM

Similar to $\langle\Lambda\rangle^{ABM}$, to determine the payoff capacity $\wp_C^{ABM}$, we start with the given values of $\mathcal{T} = 0$ and $\mathcal{F} = \frac{(\mathbb{B}\sin^2\gamma - \mathbb{C}\cos^2\gamma)}{2}$ in Eq. (21), respectively. Similar to the previous case, here also, we consider the modified energy matrix whose elements are the linear transformations of the original energy matrix elements given in Eq. (35) (see, the set of linear transformations given in Eq. (17)). Both these matrices have a one-to-one correspondence, and hence, the Nash equilibrium is preserved. So, we have the modified energy matrix as,

$$\Delta' = \begin{bmatrix} -\frac{(\mathbb{B}\sin^2\gamma - \mathbb{C}\cos^2\gamma)}{2} & -\frac{(\mathbb{B}\sin^2\gamma - \mathbb{C}\cos^2\gamma)}{2} \\ \frac{(\mathbb{B}\sin^2\gamma - \mathbb{C}\cos^2\gamma)}{2} & \frac{(\mathbb{B}\sin^2\gamma - \mathbb{C}\cos^2\gamma)}{2} \end{bmatrix}. \tag{37}$$

Both Δ in Eq. (35) and Δ' in Eq. (37) are equivalent to each other. Now, by following the algorithm given in Sec. II B 2, for $\mathbb{B} = 5.0$ and $\mathbb{C} = 2.0$, we determine the ABM payoff capacity ($\wp_C^{ABM}$), and its variation with the entanglement γ is shown in Figs. 7a, 7b. We again observe exactly the same results obtained for $\wp_C^{ABM}$ and $\wp_C^{NEM}$ in the finite and limiting values of β.

3. Analysis for payoff capacity

The analysis of the payoff capacity: $\wp_C^{NEM}$ as well as $\wp_C^{ABM}$, will be done in this subsection. From Fig. 7, for increasing values of β, we observe that for all $\gamma \to \{0, \frac{\pi}{2}, \pi\}$, i.e., for both *minimal* (i.e., $\gamma \to 0$ or π) and *maximal entanglement* (i.e., $\gamma \to \frac{\pi}{2}$), $\wp_C^{ABM} = \wp_C^{NEM} \to 0$, indicating no phase transition among the players for a unit change in *noise*. This can also be verified from the player's payoff average result (see, Fig. 6) where we see that for finite as well as limiting values of β, when $\gamma \to \{0, \frac{\pi}{2}, \pi\}$, a large fraction of players choose either *defect* (for $\gamma \to 0$ or π) or *quantum* (for $\gamma \to \frac{\pi}{2}$), and this leads to a vanishing $\wp_C$. Interestingly, in the Z-N (or, $\beta \to \infty$) limit, we observe two *first*-order phase transition peaks, as shown in Fig. 7b, at the two critical values of γ (i.e., at γ_A and γ_B) and this signifies the change in phases from *defect* to *quantum* and vice-versa at γ_A and γ_B, respectively. The values of $\gamma_{A,B}$, where we observe the phase transitions, depend on the payoffs $\mathbb{B}$ and $\mathbb{C}$ via the relation: $\gamma_{A,B} = \tan^{-1}\sqrt{\mathbb{C}/\mathbb{B}}$, and both $\mathbb{B}$ as well as $\mathbb{C}$ can induce phase transition(s).

IV. CONCLUSION

In this paper, we sought to understand the emergence of cooperative behaviour among an infinite number of players playing the quantum Prisoner's dilemma (QuPD) game by comparing a numerical technique, i.e., Agent-based modelling (ABM), with the analytical NEM method. In the *TL* of the *one-shot* game setup, we studied five different indicators, i.e., game magnetization

(μ), entanglement susceptibility (χ_γ), correlation ($\mathfrak{c}_j$), player's payoff average ($\langle\Lambda\rangle$) and payoff capacity ($\wp_C$), to understand the phase transitions occurring in QuPD. Table-I summarises the outcomes for each of the five indicators in the limiting β cases. For all the five indicators in question, we observed that *quantum* ($\mathbb{Q}$) remains the dominant strategy for a large fraction of players within a particular entanglement (γ) range (i.e., $\gamma \in [\gamma_A, \gamma_B]$). Within this γ-range, $\mathbb{Q}$ becomes the *Nash equilibrium* strategy as well as the *Pareto optimal* strategy for the players. For the payoff values $\mathbb{B} = 5.0$ and $\mathbb{C} = 2.0$, we found critical γ values: $\gamma_A = 0.5639$ and $\gamma_B = 2.5777$, within which all players play $\mathbb{Q}$. For other values of γ, i.e., $\gamma \in [0, \gamma_A) \cup (\gamma_B, \pi]$, a large fraction of players play the classical *defect* ($\mathcal{D}$). For the maximally entangled case, i.e., $\gamma = \pi/2$, we observed that the player's payoff average (corresponding to all players playing $\mathbb{Q}$) reached its maximum value.

For all five indicators, i.e., μ, χ_γ, $\mathfrak{c}_j$, $\langle\Lambda\rangle$ and $\wp_C$, in the *TL*, we observed an interesting phenomenon of two *first*-order phase transitions, namely, the change of phases (or, *strategies*) from $\mathcal{D} \to \mathbb{Q}$ (at entanglement value γ_A) and $\mathbb{Q} \to \mathcal{D}$ (at entanglement value γ_B). This result is very similar to the ones observed in Type-*I* superconductors, at a certain critical temperature and in the absence of an external field (see, Refs. [3, 21]). This also showcases the fact that for QuPD, at finite entanglement γ and *zero* noise, we observe a change in the Nash equilibrium condition from *All-*$\mathcal{D}$ to *All-*$\mathbb{Q}$ and this is marked by a *first*-order phase transition in all the five indicators. To conclude, this paper is primarily focused on mapping a *one-shot* QuPD game to the 1D-Ising chain and then numerically studying the emergence of cooperative behaviour among an infinite number of players by involving five different indicators, all of which have a thermodynamic analogue. This work can be further extended to *repeated* QuPD games, involving unitary actions/operators like *Hadamard* ($\hat{\mathbb{H}}$), etc. or other non-Unitary operators (by using modified *EWL* protocol) [9, 26].

AUTHOR DECLARATIONS

A. Conflict of Interest

The authors have no conflicts to disclose.

B. Data Availability Statement

The data that supports the findings of this study are available in the article and Appendix.

Appendix A: Python code for determining Entanglement susceptibility via ABM

Following the publication of this work, the code to determine QuPD's Entanglement susceptibility via ABM will be made available.

Appendix B: Python code for determining Correlation via ABM

Following the publication of this work, the code to determine Correlation in QuPD via ABM will be made available.

[1] M.A. Nowak, S. Coakley, *Evolution, Games, and God: The Principle of Cooperation* (2013)

[2] M. Nowak, A. Sasaki, C. Taylor *et al*, *Emergence of cooperation and evolutionary stability in finite populations*, Nature **428**, 646–650 (2004).

[3] C. Benjamin, A. Dash, *Thermodynamic susceptibility as a measure of cooperative behaviour in social dilemmas*, Chaos, **30** 093117 (2020).

[4] Jabir T. M., N. Vyas, C. Benjamin, *Is the essence of a quantum game captured completely in the original classical game?*, Physica A: Stat. Mech. and App., Volume **584**, 126360 (2021)

[5] A. Mukhopadhyay *et. al.*, *Repeated quantum game as a stochastic game: Effects of the shadow of the future and entanglement*, Physica A: Stat. Mech. and App., Volume **637**, 129613 (2024)

[6] S. Sarkar, C. Benjamin, *The emergence of cooperation in the thermodynamic limit*, Chaos **135**, 109762 (2020).

[7] S. Galam, B. Walliser, *Ising model versus normal form game*, Physica A: Statistical Mechanics and its Applications, **389:3** (2010).

[8] S. Sarkar, C. Benjamin, *Quantum Nash equilibrium in the thermodynamic limit*, Quantum Inf Process **18**, 122 (2019).

[9] J. Eisert, M. Wilkens, M. Lewenstein, *Quantum Games and Quantum Strategies*, Phys. Rev. Lett. **83**, 3077 (1999).

[10] C. Benjamin, S. Sarkar, *Triggers for cooperative behaviour in the thermodynamic limit: A case study in Public goods game*, Chaos **29**, 053131 (2019).

[11] C. Benjamin, Arjun Krishnan U.M., *Nash equilibrium mapping vs. Hamiltonian dynamics vs. Darwinian evolution for some social dilemma games in the thermodynamic limit*, Eur. Phys. J. B **96**, 105 (2023).

[12] C. Adami, A. Hintze, *Thermodynamics of evolutionary games*, Phys. Rev. E **97**, 062136 (2018).

[13] R. Tah, C. Benjamin, *Game susceptibility, Correlation and Payoff capacity as a measure of Cooperative behavior in the thermodynamic limit of some Social dilemmas*, arXiv:2401.18065 [cond-mat.stat-mech] (2024).

[14] P.M. Altrock, A. Traulsen, *Deterministic evolutionary game dynamics in finite populations*, Phys. Rev. E **80**, 011909 (2009).

[15] G.T. Landi, *Ising model and Landau theory, Undergraduate Statistical Mechanics, IFUSP - Physics Institute, University of São Paulo*, Chapter **3**, Ferromagnetism (2017).

[16] C. Benjamin, A. Dash, *Switching global correlations on and off in a many-body quantum state by tuning local entanglement*, Chaos 1 September 2023;**33 (9)**:091104.

[17] M. DeVos, D.A. Kent, *Game Theory: A Playful Introduction*, American Mathematical Society (2016).

[18] A.P. Flitney, D. Abbott, *An Introduction to Quantum Game Theory*, Fluctuation and Noise Letters, Vol. 02, No. 04, pp. **R175-R187** (2002).

[19] S. Schecter, H. Gintis, *Game Theory in Action: An Introduction to Classical and Evolutionary Models*, Princeton University Press (2016).

[20] S. Sarkar, C. Benjamin, *Entanglement renders free riding redundant in the thermodynamic limit*, Physica A: Stat. Mech. and App., Volume **521**, Pages 607-613 (2019).

[21] G. Jaeger, *The Ehrenfest Classification of Phase Transitions: Introduction and Evolution*, Arch Hist Exact Sc. **53**, 51–81 (1998).

[22] A. Sandvik, *Computational Physics lecture notes, Fall 2023, Department of Physics, Boston University*, Measuring physical observables.

[23] G. Hocky *et al.*, *Statistical Mechanics lecture notes, 2021, New York University*, Metropolis Monte Carlo for the Ising Model.

[24] R.J. Baxter, *Exactly Solved Models in Statistical Mechanics, 1982, Academic Press.*

[25] A. Bordg, Y. He, *Comment on "Quantum Games and Quantum Strategies"*, arXiv:1911.09354 [quant-ph] (2019)

[26] De He, T. Ye, *An Improvement of Quantum Prisoners' Dilemma Protocol of Eisert-Wilkens-Lewenstein*, Int J Theor Phys **59**, 1382–1395 (2020).